Generation of rapid rise current pulses in the msec range for fast compression experiments

A. Knobloch, G. Herppich

IPP 4/57 June 1968

INSTITUT FÜR PLASMAPHYSIK

GARCHING BEI MÜNCHEN

INSTITUT FÜR PLASMAPHYSIK

GARCHING BEI MÜNCHEN

Generation of rapid rise current pulses in the msec range for fast compression experiments

A. Knobloch, G. Herppich

IPP 4/57 June 1968

The contents of this report will be presented at the 5th Symposium on Fusion Technology at St. Catherine's College, Oxford, 2nd - 5th July 1968.

Die nachstehende Arbeit wurde im Rahmen des Vertrages zwischen dem Institut für Plasmaphysik GmbH und der Europäischen Atomgemeinschaft über die Zusammenarbeit auf dem Gebiete der Plasmaphysik durchgeführt.

Contents

IPP 4/57

Generation of rapid rise current pulses in the msec range for fast compression experiments

A. Knobloch, G. Herppich

June 1968

Abstract

It seems that in the field of shock heating and fast compression experiments it might be worthwhile to increase the length of discharge vessels by about one order of magnitude. In order to optimize the lumped parameter capacitive energy storage systems for such applications, the design considerations, which were briefly mentioned in Frascati in 1966,[1] have been extended. When assuming certain practical geometric arrangements and assuming the voltage dependence of the several components to be linear in a limited range, one arrives at the following equation for the primary bank generating the rapid rise:

$$\omega^2 \frac{E^*}{n} = \frac{1 - \eta}{K_s}$$

where $\omega = 2\pi$ times the discharge frequency; $\frac{E^*}{n}$ = stored energy per unit length of coil divided by the number of banks connected in series.

η = energy efficiency

K_s = storage constant

K_s consists of geometry factors and specific stress values, i.e. it is a measure of the technical standard applied. Relations for the determination of capacitor bank components as well as physical dimensions, numbers, and storage costs will be given.

The conditions for producing relatively long current pulses with the same coil which generates the rapid rise have been investigated. One arrives at relations which determine the data of the constant current source in terms of the optimized primary bank. The form of the constant current source has to be chosen according to the conditions of the special case. Some possibilities are discussed.

Introduction

Fast shock heating and compression experiments are an essential group of devices which can achieve high plasma temperatures. In these installations a major part of the technical outlay goes into energy storage. Up to now energy storage devices for such applications have been built or planned for energies up to about 10 MJ. Besides a desirable systematic review of what data can be achieved so far with lumped parameter circuits, the following investigations may also be useful for evaluating any increase of linear or toroidal compression experiments. In large installations the discharge data - only these will be discussed here - cannot be selected independently, but stand in close relation, especially for optimum design. The reasons for this are of a spatial and economic nature. This may also hold to a certain extent for the plasma data which can be obtained.

The following figures for a large fast compression experiment shall only show the order of magnitude required for studying stability and equilibrium:

density	$n \approx 10^{16} \frac{1}{cm3}$
ion temperature	$T_i \approx 10$ keV
containment time	$\tau_o \approx 10^{-4}$ sec

(As to the product $n \cdot T_o$, we are still two to three orders of magnitude from the Lawson limit). Corresponding electrical discharge data are [2] :

maximum flux density	$\hat{B} \approx 200$ kG	(1)
flux density rise	$\dot{B} \approx 10^{11} \frac{G}{sec}$	(2)
pulse duration	$\tau_o : 10^{-4} \div 10^{-3}$ sec	

With an inner coil diameter of D = 10 cm (single-turn coil) this means a coil energy per unit length of $\hat{E}^{*} \approx 1.25 \frac{MJ}{m}$ for the magnetic field rise and an initial coil voltage of U = 78.5 kV. According to pulse duration and corresponding losses, the total stored energy required can be a multiple of the above value.

1 Generation of fast current rise

This report deals essentially with the relationships between spatial arrangement and electrical discharge data of large lumped parameter capacitor energy storage systems in which the length of the load is equal to the connecting width of the storage block. In compression experiments, the load can be well approximated by an inductance. For the sake of simplicity, lossless systems are assumed, as far as the rise time interval is concerned, whereas for the constant current period the losses with and without magnetic field diffusion will be considered. [3]

1.1 Storage constant K_s

According to Fig. P 176 (top), the following relations hold for the n-times series connected capacitor bank with inductive load:

$$E_1 = \frac{1}{2} C_1 U_1^2 \qquad (3)$$

$$n \cdot E_n = E_1 \qquad (4)$$

$$U_n = f(n) \cdot U_1 \qquad (5)$$

$$U_{res} = n \cdot f(n) \cdot U_1 \qquad (6)$$

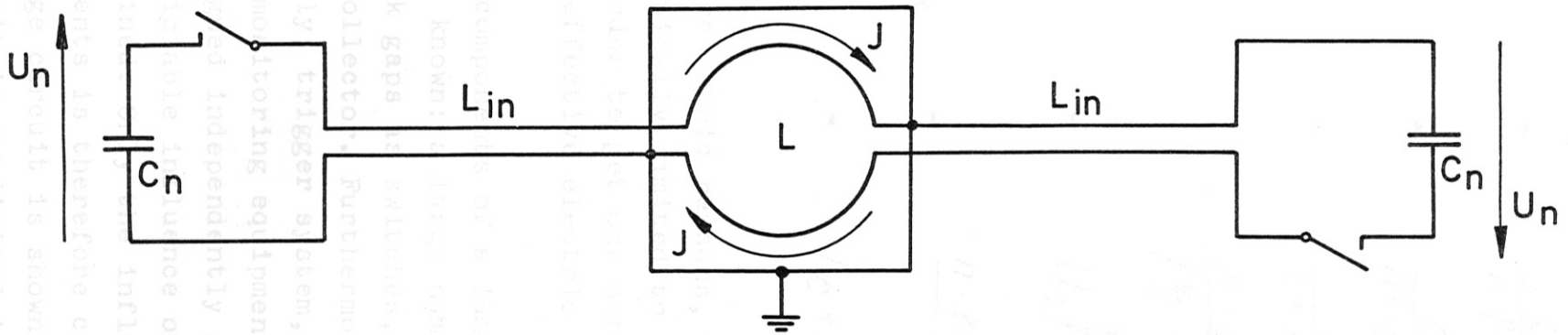

n = 2

Circuit Diagram

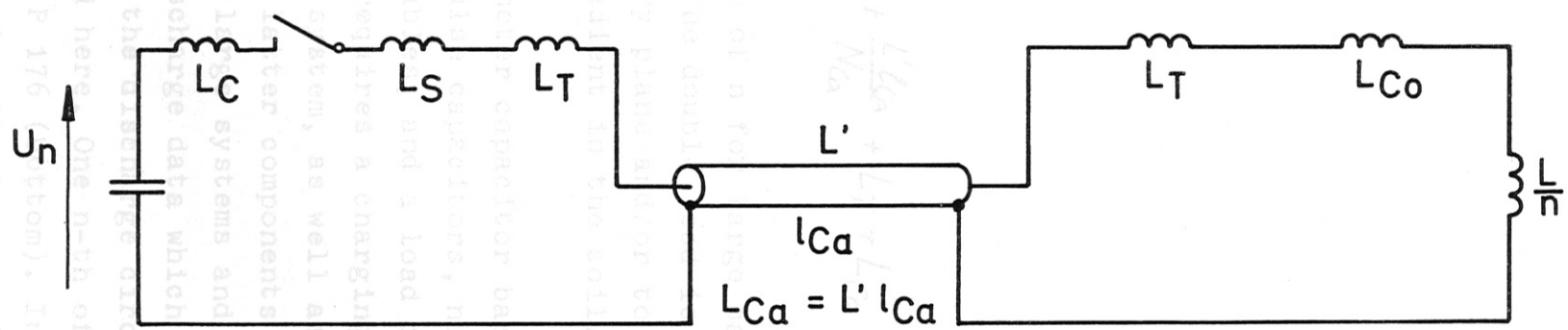

Inductance Components

Capacitive Energy Storage
inductive load, n banks in series

$$C_n = \frac{C_1}{n f^2(n)} \qquad (7)$$

$$C_{res} = \frac{C_1}{n^2 \cdot f^2(n)} \qquad (8)$$

$$\eta = \frac{L}{L + n L_{in}} \qquad (9)$$

$$\omega = \frac{n \cdot f(n)}{\sqrt{\frac{L}{\eta} C_1}} \qquad (10)$$

$$\hat{J} = U_1 \sqrt{\frac{\eta C_1}{L}} \qquad (11)$$

$$\dot{J}_{max} = \frac{n \cdot f(n) \cdot U_1 \cdot \eta}{L} \qquad (12)$$

$$L_{in} = L_C + L_S + L_T + \frac{L' l_{Ca}}{N_{Ca}} + L_T + L_{Co} \qquad (13)$$

For geometric reasons, the value of n for large banks is practically limited to 1 or 2. The double feed is applied in order to get one more symmetry plane and/or to increase the effective electric field gradient in the coil.

The components of a lumped parameter capacitor bank are well known: a large number of pulse capacitors, numerous spark gaps as switches, pulse cables, and a load connector or collector. Furthermore, one requires a charging power supply, trigger system, control system, as well as measuring and monitoring equipment. These latter components can be designed independently even for large systems and have negligiable influence on the discharge data which can be attained. Only the influence of the discharge circuit elements is therefore calculated here. One n-th of the discharge circuit is shown in Fig. P 176 (bottom). In fact the circuit is subdivided into N_C/n circuit elements (N_C = total number of capacitors) for safety reasons and in order to achieve a sufficient energy efficiency.

For f (n) = 1 we have

$$\omega = \frac{n}{\sqrt{\frac{L}{\eta} C_1}} = \frac{\sqrt{1-\eta}}{\sqrt{\frac{L_{in}}{n} \cdot C_1}} \qquad (14)$$

With A as connecting length of the load, the stored energy per unit load length is

$$E^* = \frac{E_1}{A} \qquad (15)$$

At first we know nothing about L_{in} in general. But it is reasonable to make the following assumptions:

1. Because of the insulation distances, L_{in} will be proportional to the operating voltage U_n - at least in a certain range.

2. As the storage block structure will be homogeneous along the load length, the following equation will hold:

$$L_{in} \sim \frac{1}{A} \qquad (16)$$

3. Furthermore, all bank inductances will be proportional to one geometric dimension of the storage block. As one dimension, namely A, is fixed, there remains:

$$L_{in} \sim \sqrt{E_n} \sim U_n \qquad (17)$$

So we have from the three assumptions

$$L_{in} \sim U_n^2 \cdot \frac{1}{A} \tag{18}$$

$$\omega = \sqrt{\frac{1-\eta}{K_s \frac{E^*}{n}}} \tag{19}$$

$$\omega^2 \frac{E^*}{n} = \frac{1-\eta}{K_s} \tag{20}$$

The last equation is of fundamental importance insofar as all optimized inductively loaded capacitor banks (with lumped parameters) are approximately described. The optimization concerns the choice of η from the point of view of optimum design, and a minimum value of the storage constant K_s.

It should be noted that direct calculation of L_{in} in terms of the geometric lengths and the electrical stress figures also leads almost direct to the equation (20). But if this formula is already known one gets a clear formal treatment and finds in addition some plausible definitions.

The storage constant K_s is a kind of a measure of the technical standard of a capacitive energy storage device. It is a function of the material constants, specific stress values, and major design characteristics.

Conversely one is able to make direct comparisons of different storage systems with known figures for $\frac{E^*}{n}$, ω, and η by means of the resulting K_s. The smaller K_s is, the "better" is the capacitor bank. Naturally, all kinds of capacitor bank performance with higher values than $K_{s_{min}}$ are possible and in certain cases, e.g. for bias fields, even necessary.

1.2. Choice of energy efficiency

Assuming a single-turn cylindrical coil of inner diameter D as the load, we have for the total bank energy per unit load length:

$$E^* = \frac{1}{2}\mu_0 \frac{\pi}{4} \frac{D^2}{A} \frac{B^2}{\mu_0} A^2 \frac{1}{\eta} \cdot \frac{1}{A} = \frac{\pi}{8\mu_0\eta} D^2 B^2 \qquad (21)$$

and consequently

$$BD = \sqrt{\frac{8\mu_0}{\pi}\eta} \cdot \sqrt{E^*} = \sqrt{\frac{8\mu_0\eta}{\pi}} \sqrt{\frac{E^*}{n}} \cdot \sqrt{n} \qquad (22)$$

From this equation we have the initial voltage gradient

$$\frac{U_L}{\pi D} = \frac{\omega}{4} BD = \sqrt{\frac{\mu_0\eta}{2\pi}}\, \omega \sqrt{\frac{E^*}{n}} \cdot \sqrt{n} \qquad (23)$$

With equation (20) both quantities can be expressed in terms of ω, η :

$$BD = \sqrt{\frac{8\mu_0\eta}{\pi}} \sqrt{\frac{1-\eta}{K_S}} \sqrt{n} \cdot \frac{1}{\omega} \qquad (24)$$

$$\frac{U_L}{\pi D} = \sqrt{\frac{\mu_0\eta}{2\pi}} \sqrt{\frac{1-\eta}{K_S}} \sqrt{n} \qquad (25)$$

Therefore, disregarding the technical outlay required and with given discharge frequency, the maximum values of $\hat{B}$ and $\dot{B}$ will be attained for $\eta = \frac{1}{2}$. More economical conditions will result from optimization with respect to $\hat{B} \cdot \dot{B}$ (Poynting vector) or $\hat{B} \cdot \sqrt{\dot{B}}$. The latter value characterizes to a certain extent the plasma temperature which can be reached. Figure P 177 shows the optimization of η for the three cases mentioned. According to equation (20) all optimum capacitor banks for $(\hat{B} \cdot \dot{B})_{max}$ are described by

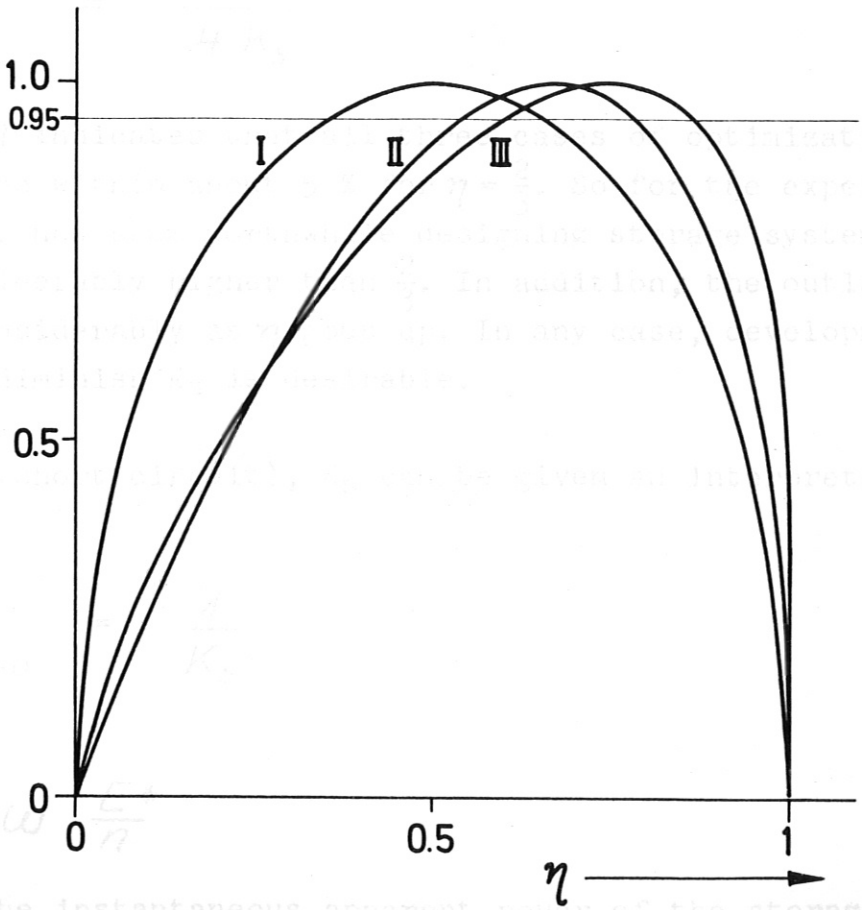

I : $2{,}0\sqrt{\eta(1-\eta)}$, $\eta_{opt} = \frac{1}{2}$ for $\dot{B}_{max}$

II : $2{,}6\,\eta\sqrt{(1-\eta)}$, $\eta_{opt} = \frac{2}{3}$ for $(\hat{B}\cdot\dot{B})_{max}$

III : $3{,}08\sqrt[4]{\eta^3(1-\eta)}$, $\eta_{opt} = \frac{3}{4}$ for $(\hat{B}\sqrt{\dot{B}})_{max}$

Capacitive Energy Storage

inductive load, optimum energy efficiency for different optimization quantities

$$\omega^2 \cdot \frac{E^*}{n} = \frac{1}{3 \cdot K_s} \tag{26}$$

whereas maximum $\hat{B}\sqrt{\dot{B}}$ requires

$$\omega^2 \cdot \frac{E^*}{n} = \frac{1}{4 \cdot K_s} \tag{27}$$

Figure P 177 indicates that all three cases of optimization are fulfilled within about 5 % for $\eta = \frac{2}{3}$. So for the experiment it does not seem worthwhile designing storage systems with η considerably higher than $\frac{2}{3}$. In addition, the outlay will increase considerably as η goes up. In any case, development tending to diminish K_s is desirable.

With $\eta = 0$ (short circuit), K_s can be given an interpretation. We have

$$\left(\omega^2 \frac{E^*}{n}\right)_{\eta=0} = \frac{1}{K_s} \tag{28}$$

and

$$\frac{P^*}{n} = \omega \frac{E^*}{n} \tag{29}$$

with $\frac{P^*}{n}$ as the instantaneous apparent power of the storage system. Thus $\frac{1}{K_s}$ is the maximum rise of the apparent power for the short-circuited energy store.

1.3 Energy storage geometry

In order to get general design relations for large capacitor energy storage systems, we have to fix, among other things the geometric arrangement.

We assume the energy storage block to be cubic in form and subdivided into tiers, ranks and files containing the single capacitors, spark gaps, and pulse cables.

The space requirements for the auxiliary equipment, such as charging trigger and control devices, will be taken into account by space factors. The pulse cables run horizontally from the capacitor units to the load side of the storage block, where they are connected, e.g. via plug-in contacts, to the so-called collector. Having plug-in contacts here, the storage block itself may possibly be built with the ranks in a sort of slide-in module technique, which helps to avoid the usual service passages and increases the energy package density roughly by a factor of two. This solution is not possible, of course, with several systems in tandem.

The collector design has an important influence on the discharge data. We assume a special configuration [4] which has rather low inductance. The inductance value rises very weakly with the number of cables connected. Figure P 178 shows the principle of the arrangement for a single-fed coil. The arrangement of storage block and collector including the single-turn coil is shown in Fig. P 179. This configuration is possible for n = 1 and n = 2. (Cases with n > 2 involve considerable geometric complications.)

Each cube with the dimensions $\frac{H}{e}$, $\wp\frac{A}{r}$, $\frac{T}{z}$ contains one capacitor unit including spark gap (s) and auxiliary equipment. Figure P 180 shows the arrangement of the single cube. The cubic capacitor has strip line connectors. One layer of pulse cable terminals lies on the capacitor and the terminal length is equal to or smaller than the capacitor length. Next to the capacitor is the main gap, e.g. a pressurized air gap. A crowbar switch adjacent to the main gap can be connected across the cable terminals by means of a further connector plate lying across the cable terminals. This additional plate would also be practical without any crowbar switch because it simplifies insulation in the terminal range. The remaining space of the cube is filled with charging resistors, the shorting breaker, spark gap auxiliary equipment, and monitoring devices.

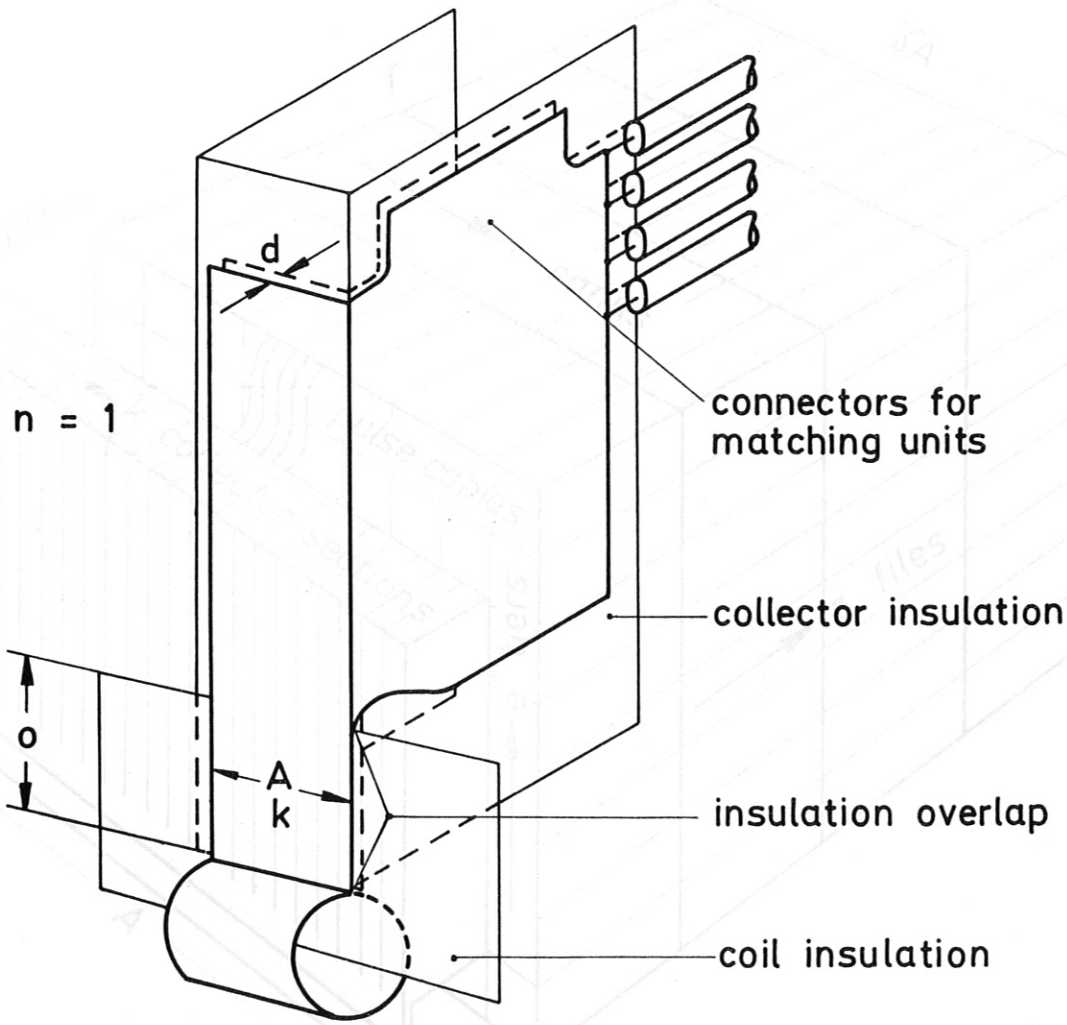

Capacitive Energy Storage
inductive load - collector section.

P 178

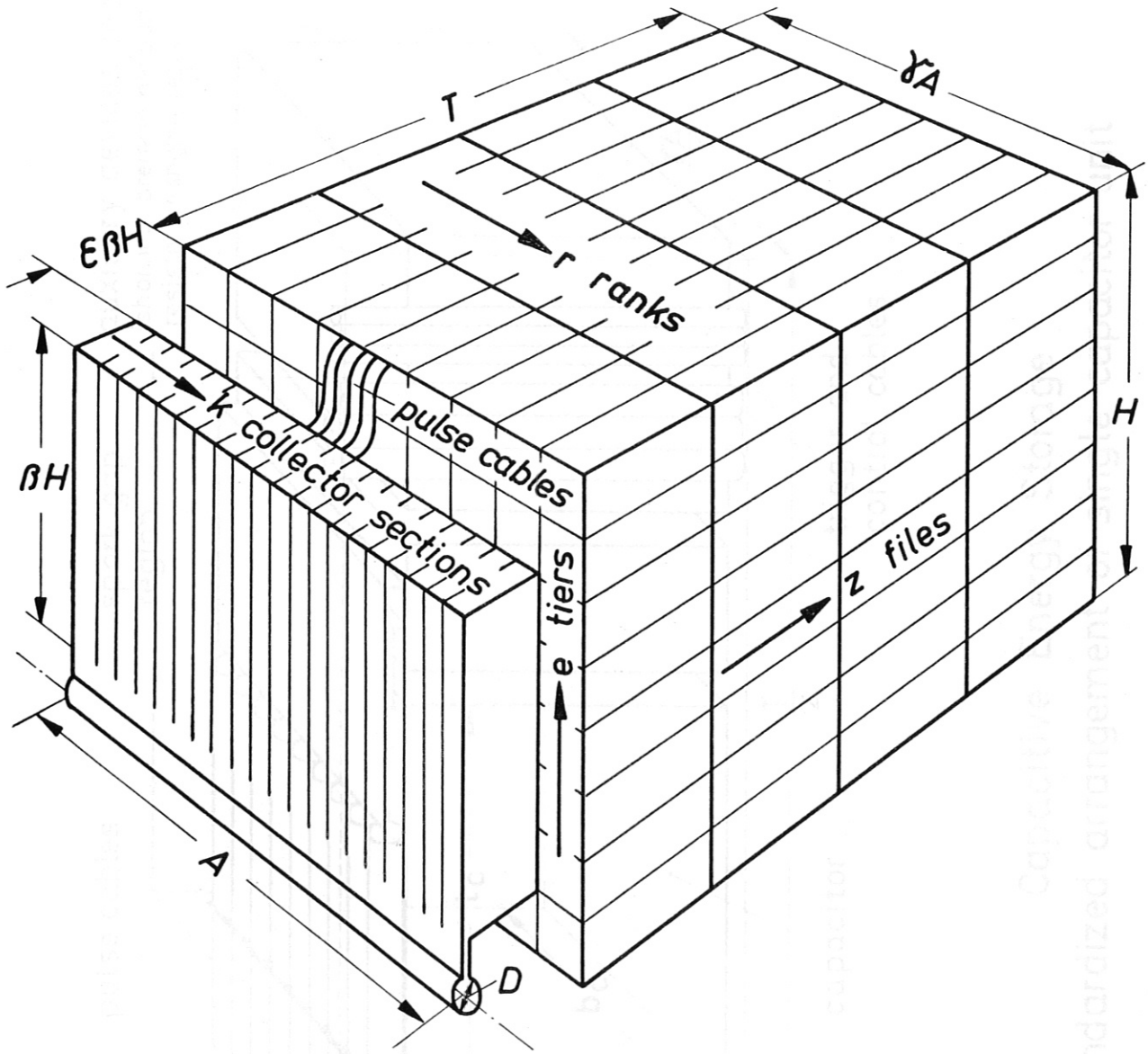

Capacitive Energy Storage
Standardized arrangement of storage block and collector P 179

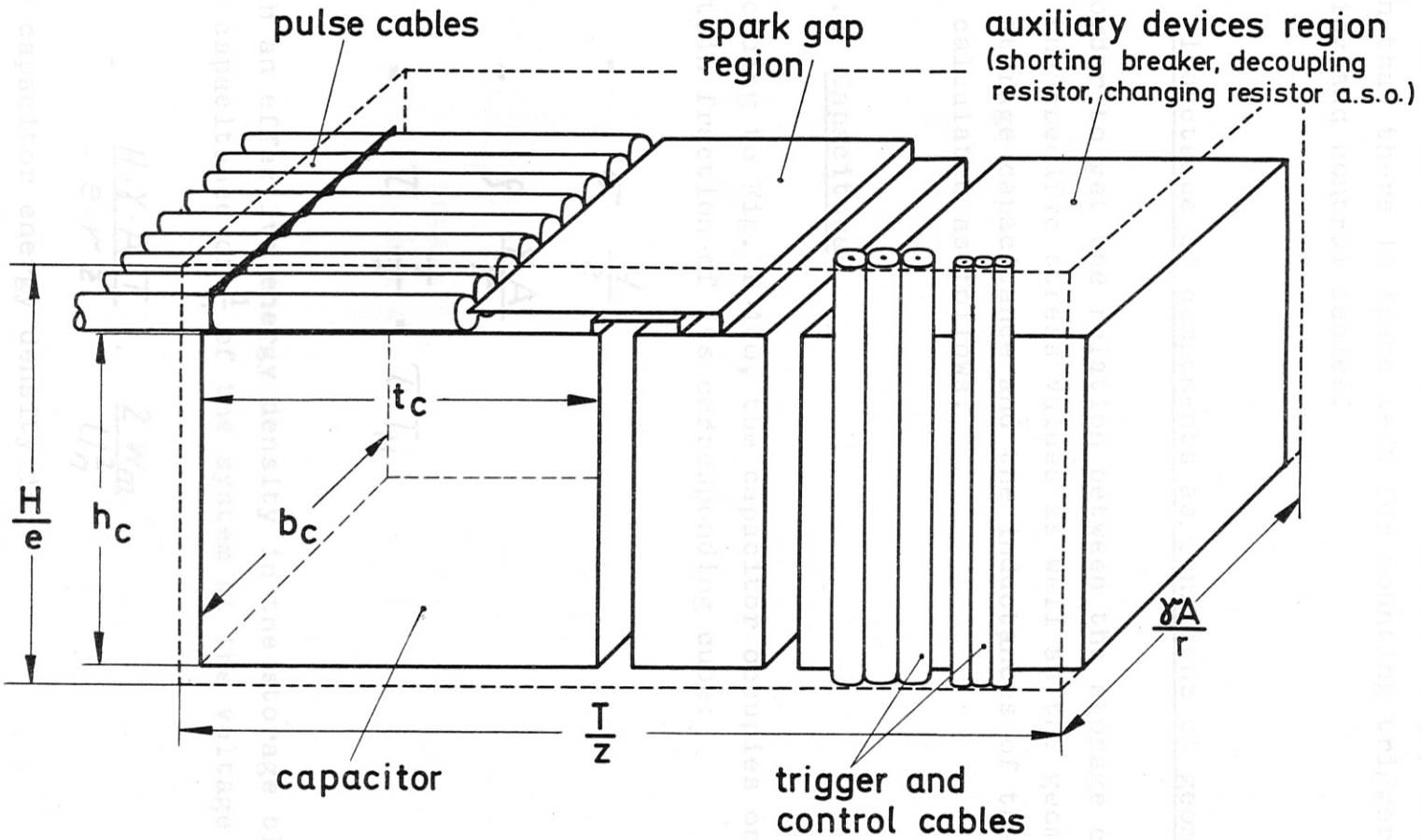

Capacitive Energy Storage
Standardized arrangement of single capacitor unit

The widths of the capacitor case and spark gap case are such that there is space left for mounting trigger, monitoring and control cables.

1.4 Inductance of components as functions of geometry

In order to get the relation between the storage constant and the specific stress values as well as the geometry factors, the storage capacitance and the inductances of the components are calculated as follows.

1.4.1 Capacitors

According to Fig. P 180, the capacitor occupies only a certain fraction of its corresponding cube:

$$h_C = \sigma \frac{H}{e} \tag{30}$$

$$b_C = \varrho \frac{\gamma A}{r} \tag{31}$$

$$t_C = \tau \frac{T}{z} = \tau T_M \tag{32}$$

With an effective energy density in the storage block w_m, the capacitance of $\frac{1}{n}$ of the system at the voltage U_n is

$$C_E = \frac{H \cdot \gamma \cdot A \cdot T}{e \cdot r \cdot z} \cdot \frac{2 w_m}{U_n^2} \tag{33}$$

The capacitor energy density is

$$w_C = \frac{w_m}{\sigma \cdot \varrho \cdot \tau} \tag{34}$$

The capacitor reel inductance is taken to be proportional to the capacitor height and length, a factor ξ being included to allow for the inductance reduction due to series and parallel connection of the reels. The width of the cable layer is equal to the capacitor width. Thus the inductances of a single capacitor and its cable connection are approximately

$$L_{CE} + L_{TE} = \mu_0 \frac{\frac{D_{Ca}}{8}\tau\frac{T}{z} + \frac{1}{3}\sigma\frac{H}{e}\frac{\tau T}{z}\xi}{\varrho\frac{\gamma A}{r}} \tag{35}$$

Consequently, the total inductance for $\frac{1}{n}$ of the system (capacitors and cable connections) will be

$$L_C + L_T = \frac{L_{CE}+L_{TE}}{e\cdot r\cdot z} = \mu_0 \frac{\frac{D_{Ca}}{8}\tau T + \frac{1}{3}\sigma\tau HT\xi\frac{1}{e}}{\varrho\gamma A e z^2} \tag{36}$$

1.4.2 Spark gaps

The definition of the main spark gap is based on a design corresponding to [5], which describes a low-inductance multiple arc pressurized spark gap with an inductance L_o at a voltage U_o and a width b_o. Thus we have for a single spark gap

$$L_{SE} = L_o \frac{b_o\cdot r}{\varrho\cdot\gamma\cdot A}\cdot\frac{U_n}{U_o} \tag{37}$$

the voltage dependence also being taken as linear. For all gaps in $\frac{1}{n}$ of the store it follows that

$$L_S = L_o \frac{U_n}{U_o}\cdot\frac{b_o}{\varrho\gamma A}\cdot\frac{1}{z\cdot e} \tag{38}$$

As can be seen from Fig. P 180, there is a maximum of σ because of space requirements of the pulse cables of adjacent units running over the units of the first file.

$$\sigma \leq 1 - \frac{z\cdot e\cdot D_{Ca}}{H} \tag{39}$$

In cases where a power crowbar device is connected by cables to every unit, the limitation of σ holds for all units. The remaining geometry factors according to equations (31) and (32) are chosen to be about

$$\varrho \leq 1 \tag{40}$$

$$\tau \approx 0{,}5 \tag{41}$$

1.4.3 Pulse cables

For calculating the inductance, all the cables of one $\frac{1}{n}$ of the storage system are taken as having the average length $l_{Ca} = l_o + l_m$. l_o stands for the average cable length between collector and storage block, l_m denotes the average length of the cables in the bank block. Therefore we have

$$l_o = \left(\varepsilon\beta + \frac{1-\beta}{2}\right) H + \frac{\gamma-1}{2} A \tag{42}$$

where β and γ are defined in Fig. P 179 and ε allows for the fact that $l_o \neq 0$ for $\beta = 1$, $\gamma = 1$. A good approximation is

$$\varepsilon\beta = 0{,}1 \tag{43}$$

Furthermore, we have

$$l_m = T \frac{z-1}{2 \cdot z} \tag{44}$$

Consequently, the average inductance of a single cable is

$$L_{CaE} = L' \left[\left(\varepsilon\beta + \frac{1-\beta}{2}\right) H + \frac{\gamma-1}{2} A + \frac{z-1}{2z}\right] \tag{45}$$

with L' for the inductance per unit length.

According to the foregoing relations, the number of cables in $\frac{1}{n}$ of the storage system is

$$N_{Ca} = \frac{\varrho \cdot \gamma \cdot A \cdot e}{D_{Ca}} z \tag{46}$$

and the resulting cable inductance

$$L_{Ca} = \frac{L_{CaE}}{N_{Ca}} \tag{47}$$

We have a second definition equation for the number of cables which is based on the rated maximum current per cable J^*:

$$N_{Ca} = \frac{\alpha}{J^*} \sqrt{\frac{2 E_1}{L}} \cdot \frac{1}{\sqrt{1 + \frac{n L_{io}}{L}}} \tag{48}$$

with $\alpha \gtrsim 1$. With equation (46), we get a defining equation for the number of tiers

$$e = \frac{D_{Ca}}{\gamma \cdot A \cdot \varrho \cdot z} \cdot \frac{\alpha}{J^*} \sqrt{\frac{2 E_1}{L}} \frac{1}{\sqrt{1 + \frac{n L_{io}}{L}}} \tag{49}$$

1.4.4 Collector

The collector inductance is composed of the precollector part and a part for the overlap region of the coil insulation with the collector insulation (see Fig. P 178). We have to add the inductance of the cable connections, which is assumed to be roughly the same as at the capacitor end. With k as the number of single precollectors, we get for the collector and cable connection inductance per $\frac{1}{n}$ of the system

$$L_{Co} + L_T = \mu_0 d \left(\frac{1}{k} + \frac{\lambda \cdot o}{A} \right) + \frac{\mu_0 D_{Ca} \tau \tau}{8 \varrho \gamma A e z^2} \tag{50}$$

λ takes into account the actual design of the overlap and the transition towards the coil.

1.5 Characteristic data of system

The sum of the component inductances calculated above gives the inductance of $\frac{1}{n}$ of the system:

$$L_{in} = \frac{\frac{D_{Ca}}{8}\tau T + \frac{1}{3}\sigma\tau H T \xi \frac{1}{e}}{\varrho \gamma A e z} \quad \text{capacitors + cable connect.} \tag{51}$$

$$+ L_0 \frac{U_n}{U_0} \frac{b_0}{\varrho \gamma A} \frac{1}{z \cdot e} \quad \text{spark gaps}$$

$$+ \frac{D_{Ca}}{\varrho \gamma A e z} \cdot L' \left[\left(\epsilon\beta + \frac{1-\beta}{2} \right) H + \frac{\gamma - 1}{2} A + \frac{z-1}{2z} T \right] \quad \text{cables}$$

$$+ \mu_0 d \left(\frac{1}{k} + \frac{\lambda_0}{A} \right) + \mu_0 \frac{e D_{Ca} \tau T}{8 \varrho \gamma A} \quad \text{collector + cable connect.}$$

where e has already been defined by equation (49). It is practical to introduce now the following relations for the

cable outer diameter

$$D_{Ca} = C_{Ca} U_n \tag{52}$$

insulation overlap length

$$o = C_o U_n \tag{53}$$

insulation thickness

$$d = C_d U_n \tag{54}$$

max. current per cable

$$J^* = C_i \cdot U_n \tag{55}$$

number of precollectors

$$k = \frac{A\sqrt{f_{Co}}}{D_{Ca}} \tag{56}$$

with f_{Co} as space factor for the collector-cable connection area.

collector-cable connection area

$$\beta H A = \frac{N_{Ca} D_{Ca}^2}{f_{Co}} \tag{57}$$

total volume of storage block (s)

$$nYAHT = \frac{E_1}{w_m} \tag{58}$$

dimension quotient

$$R = \frac{H}{T} \tag{59}$$

After some intermediate calculations, we have for the relative source inductance of the system

$$1-\eta = \frac{\mu_0 \tau \xi c_i^2 \rho}{6 \gamma C_{Ca}^2 \alpha^2 w_m} + \omega \frac{c_i}{\alpha}\left[\left(\frac{\mu_0 \tau}{4} - \frac{L'}{2}\right) T_H + L_0 \frac{b_0}{U_0 C_{Ca}} + L' \frac{\gamma-1}{2} A\right] \tag{60}$$

$$+ \omega \frac{c_i}{\alpha} \frac{\sqrt{\frac{E^*}{n}}}{\sqrt{\gamma w_m}} \left\{\left[\mu_0 C_d \frac{\beta\sqrt{f_{Co}}}{C_{Ca}} + \left(\epsilon\beta + \frac{1-\beta}{2}\right) L'\right]\sqrt{R} + \left[\frac{L'}{2} - \frac{\mu_0}{3}\tau\xi\right]\frac{1}{\sqrt{R}}\right\}$$

$$+ 2\mu_0 \lambda C_d C_0 \omega^2 \frac{E^*}{n}$$

The term in brackets depending on R can be optimized to become a minimum for

$$R_{opt} = \frac{\frac{L'}{2} - \frac{\mu_0}{3}\tau\xi}{\mu_0 C_d \frac{\beta\sqrt{R_{Co}}}{C_{Ca}} + \left(\varepsilon\beta + \frac{1-\beta}{2}\right)L'} = \frac{Y}{X} \qquad (61)$$

The bracket term can be written as

$$\{\}_{opt} = 2\sqrt{XY}\left\{\frac{1}{2}\sqrt{\frac{R}{R_{opt}}} + \frac{1}{2}\sqrt{\frac{R_{opt}}{R}}\right\} \qquad (61a)$$

Figure P 181 shows the influence of a deviation from R_{opt} on the value of the bracket term.

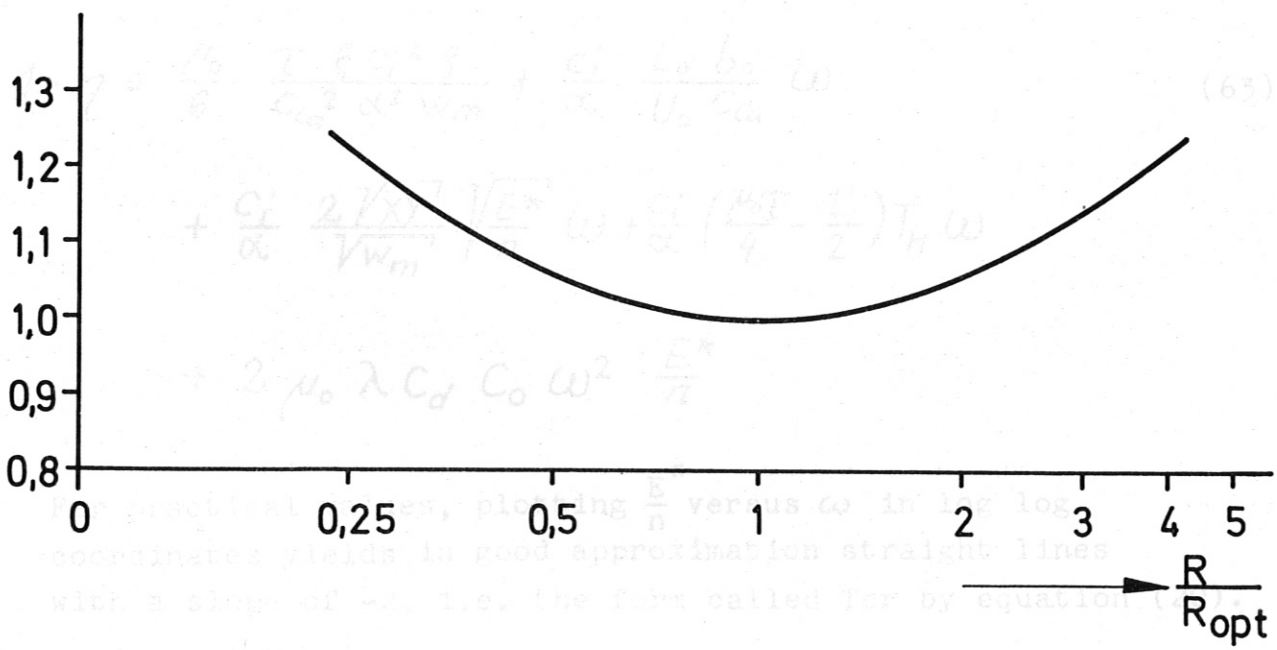

P 181

For $R = R_{opt}$ we get

$$1-\eta = \frac{\mu_0 \tau \xi c_i^2 \varrho}{6 \gamma C_{Ca}^2 \alpha^2 w_m} + \frac{c_i}{\alpha}\left\{\frac{L_0 b_0}{U_0 C_{Ca}} + L' \frac{\gamma-1}{2} A\right\} \omega \qquad (62)$$

$$+ \frac{c_i}{\alpha} \frac{2\sqrt{XY}}{\sqrt{\gamma w_m}} \sqrt{\omega} \frac{E^*}{n} + \frac{c_i}{\alpha}\left(\frac{\mu_0 \tau}{4} - \frac{L'}{2}\right) T_H \omega$$

$$+ 2 \mu_0 \lambda C_d C_0 \omega^2 \frac{E^*}{n}$$

Equation (62) indicates that especially for small A the relative source inductance can be lowered by increasing $\gamma > 1$ (see corresponding cases in Fig. P 184). For more general considerations the load coil length is an arbitrary value and γ has to be taken as 1. Thus we have

$$1-\eta = \frac{\mu_0}{6} \frac{\tau \xi c_i^2 \varrho}{C_{Ca}^2 \alpha^2 w_m} + \frac{c_i}{\alpha} \frac{L_0 b_0}{U_0 C_{Ca}} \omega \qquad (63)$$

$$+ \frac{c_i}{\alpha} \frac{2\sqrt{XY}}{\sqrt{w_m}} \sqrt{\frac{E^*}{n}} \omega + \frac{c_i}{\alpha}\left(\frac{\mu_0 \tau}{4} - \frac{L'}{2}\right) T_H \omega$$

$$+ 2 \mu_0 \lambda C_d C_0 \omega^2 \frac{E^*}{n}$$

For practical values, plotting $\frac{E^*}{n}$ versus ω in log log coordinates yields in good approximation straight lines with a slope of -2, i.e. the form called for by equation (20).

The formal adaptation of equation (63) to equation (20) is achieved by the following plausible definitions.

Equation (63) contains three quantities, namely α, b_0 and T_M, which can be additionally defined and whose formal appearance in the equation suggest such a definition.

α can be interpreted as indicating that the cable stress varies according to the kind of performance of a certain energy storage system. One can easily show that the maximum current of an inductively loaded capacitor bank (source inductance L_{in}) varies as

$$\hat{J} = U_1 \sqrt{\frac{C_1}{L_{in}}} \sqrt{1-\eta} \tag{64}$$

So we write

$$\frac{C_i}{\alpha} = \frac{C_i}{\alpha_k} \sqrt{1-\eta} \tag{65}$$

α_K is the value of α for short-circuit conditions (η = o) e.g. when α = 1 for $\eta = \frac{2}{3}$. Because of equation (20) we have

$$\frac{C_i}{\alpha} = \frac{C_i}{\alpha_k} \cdot \sqrt{K_S}\, \omega \sqrt{\frac{E^*}{n}} \tag{66}$$

It is also formally consequent and plausible to put

$$T_H = K_T \sqrt{\frac{E^*}{n}} \tag{67}$$

$$b_o = K_b \sqrt{\frac{E^*}{n}} \tag{68}$$

This means that the size of the cubes will increase with the energy per unit length of load.

Now we get from equation (63)

$$1-\eta = \left\{ \frac{\mu_o}{6} \frac{\tau\, \xi\, \varrho}{C_{ca}^2 w_m} \cdot \left(\frac{C_i}{\alpha_k}\right)^2 K_S + \frac{L_o K_b}{U_o C_{ca}} \frac{C_i}{\alpha_k} \sqrt{K_S} + \right. \tag{69}$$

$$+ \frac{2\sqrt{xy}}{\sqrt{w_m}} \frac{C_i}{\alpha_k} \sqrt{K_S} + \left(\frac{\mu_o \tau}{4} - \frac{L'}{2}\right) K_T \cdot \frac{C_i}{\alpha_k} \sqrt{K_S} +$$

$$\left. + 2\, \mu_o \lambda\, C_d\, C_o \right\} \omega^2 \frac{E^*}{n}$$

Together with equations (20) and (66), this yields K_S:

$$K_S = \frac{C}{A} + \frac{1}{2}\left(\frac{B}{A}\right)^2 \left[1 + \sqrt{1 + \frac{4AC}{B^2}}\right] \tag{70}$$

$$A = 1 - \frac{\mu_0}{6} \frac{\tau \xi \varrho c_i^2}{w_m c_{ca}^2 \alpha_k^2} \tag{71}$$

$$B = \frac{c_i}{\alpha_k}\left[\frac{L_o K_b}{U_o c_{ca}} + \frac{2\sqrt{XY}}{\sqrt{w_m}} + \left(\frac{\mu_0}{4}\tau - \frac{L'}{2}\right) K_T\right] \tag{72}$$

$$C = 2 \mu_o \lambda c_d c_o \tag{73}$$

1.6 Relative component inductances

After K_S has been calculated, the contributions of the components according to Fig. P 176 to the system inductance can be determined from the bracket terms of equation (69):

$$1 - \eta = \frac{n\,(L_c + L_s + 2L_T + L_{ca} + L_{co})}{L + nL_{in}} \tag{73a}$$

$$\frac{nL_c}{L + nL_{in}} = \frac{\mu_o \tau \xi \varrho c_i^2}{6 c_{ca}^2 w_m \alpha_k^2} K_S \omega^2 \frac{E^*}{n} - \frac{\mu_o \tau \xi c_i \sqrt{\frac{X}{Y}}}{3\alpha_k \sqrt{w_m}} \sqrt{K_S'} \omega^2 \frac{E^*}{n} \tag{73b}$$

$$\frac{nL_s}{L + nL_{in}} = \frac{L_o K_b c_i}{U_o c_{ca} \alpha_k} \sqrt{K_S'} \omega^2 \frac{E^*}{n} \tag{73c}$$

$$\frac{2nL_T}{L + nL_{in}} = \frac{\mu_o \tau K_T c_i}{4\alpha_k} \sqrt{K_S'} \omega^2 \frac{E^*}{n} \tag{73d}$$

$$\frac{n L_{ca}}{L+nL_{in}} = \left\{ \frac{L' c_i}{\alpha_K \sqrt{W_m}} \left[\left(\varepsilon\beta + \frac{1-\beta}{2}\right)\sqrt{\frac{Y}{X}} + \frac{1}{2}\sqrt{\frac{X}{Y}} \right] - \frac{L' c_i K_T}{2\alpha_K} \right\} \sqrt{K_s}\,\omega^2 \frac{E^*}{n} \qquad (73e)$$

$$\frac{n L_{co}}{L+nL_{in}} = \frac{\mu_0 c_i c_d \beta \sqrt{f_{co}} \sqrt{\frac{Y}{X}}}{c_{ca}\alpha_K \sqrt{W_m}} \sqrt{K_s}\,\omega^2 \frac{E^*}{n} + 2\mu_0 \lambda c_d c_o \omega^2 \frac{E^*}{n} \qquad (73f)$$

A typical percentage subdivision of the source inductance for usual specific stress values is given in Table I.

Table I

components	% bank internal inductance
capacitors	7.2
spark gaps	5.6
cables	18.8
cable connections	10.3
collector	58.1
	100.0

The prevailing term comes from the collector insulation overlap region.

1.7 Dimensioning relations

After some intermediate calculations, we get from the above derived equations some dimensioning relations for capacitive energy storage.

Equation (34) yields

$$\frac{W_m}{W_c} = \varsigma\tau \left(1 - \frac{2 c_{ca}^2 \alpha_K}{\varsigma c_i \sqrt{K_s}} \sqrt{\frac{X}{Y} W_m} \right) \qquad (74)$$

for the relation of average energy density in the storage block to capacitor energy density.

The number of tiers is according to equation (49), with $\gamma = 1$:

$$e = \frac{2 C_{Ca} K_T \sqrt{2 w_m} \alpha_K \sqrt{\frac{Y}{X}}}{D \varrho \sqrt{\pi \mu_0} C_i \sqrt{K_S}} \sqrt{\eta} \sqrt{n} \frac{1}{\omega} \tag{75}$$

The storage block height becomes

$$H = \sqrt{\frac{Y}{X w_m}} \sqrt{\frac{E^*}{n}} = \sqrt{\frac{Y}{X w_m}} \frac{1}{\sqrt{K_S}} \sqrt{1-\eta} \frac{1}{\omega} \tag{76}$$

and therefore the height of one tier is

$$h_e = \frac{H}{e} = \frac{D \varrho \sqrt{\pi \mu_0} C_i}{2 C_{Ca} K_T \sqrt{2} w_m \alpha_K} \sqrt{\frac{1-\eta}{\eta}} \frac{1}{\sqrt{n}} \tag{77}$$

With the abbreviation

$$\frac{\varrho \sqrt{\pi \mu_0}}{2 \sqrt{2} C_{Ca}} C_i = \bar{C}_i \tag{78}$$

we have

$$e = \frac{\alpha_K K_T \sqrt{w_m \frac{Y}{X}}}{D \bar{C}_i \sqrt{K_S}} \sqrt{\eta} \sqrt{n} \frac{1}{\omega} \tag{79}$$

$$h_e = \frac{D \bar{C}_i}{\alpha_K K_T w_m} \sqrt{\frac{1-\eta}{\eta}} \frac{1}{\sqrt{n}} \tag{80}$$

Consequently, the tier height does not depend on the discharge data. We introduce g^* as the number of capacitor units per unit length of one file (see Fig. P 179). So we have for the energy of a single capacitor unit:

$$E_c = \frac{E^*}{n g^* e z} = \frac{D \bar{C}_i}{\alpha_K g^* \sqrt{K_S}} \cdot \frac{1-\eta}{\sqrt{\eta}} \frac{1}{\sqrt{n}} \frac{1}{\omega} \tag{81}$$

From equation (25) we get the charging voltage

$$U_n = \pi D \sqrt{\frac{\mu_0}{2\pi}} \frac{1}{\sqrt{K_S}} \sqrt{\frac{1-\eta}{\eta}} \frac{1}{\sqrt{n}} \tag{82}$$

which depends only on the technical standard characterized by K_S.

Equations (81) and (82) yield the capacitance of one capacitor unit

$$C_E = \frac{4\,\bar{c}_i \sqrt{K_S}}{\pi \mu_0 D\, g^* \alpha_K} \sqrt{\eta} \sqrt{n} \frac{1}{\omega} \tag{83}$$

The total number of capacitor units per unit length of load is

$$N_c^* = \frac{E^*}{E_c} = \frac{g^* \alpha_K}{D\,\bar{c}_i \sqrt{K_S}} \sqrt{\eta}\, n^{\frac{3}{2}} \frac{1}{\omega} \tag{84}$$

and the total number of cables per unit length of load with equation (82)

$$N_{Ca}^* = N_c^* \frac{g}{g^* C_{Ca} U_n} = \frac{\sqrt{2}\, g\, \alpha_K}{\sqrt{\pi \mu_0}\, \bar{c}_i D^2 C_{Ca} \sqrt{1-\eta}} \frac{\eta}{\sqrt{1-\eta}}\, n^2 \frac{1}{\omega} \tag{85}$$

The average cable length according to equation (45) is for $\gamma = 1$:

$$l_{Ca} = \left(\varepsilon\beta + \frac{1-\beta}{2}\right) H + \frac{z-1}{2z} T \tag{86}$$

Therefore we have (without cable terminals)

$$l_{Ca} = \left\{ \frac{\left[\left(\varepsilon\beta + \frac{1-\beta}{2}\right) \cdot \sqrt{\frac{Y}{X}} + \frac{1}{2}\sqrt{\frac{X}{Y}}\right]}{\sqrt{W_m}} - \frac{K_T}{2} \right\} \frac{1}{\sqrt{K_S}} \frac{\sqrt{1-\eta}}{\omega} \tag{87}$$

and the total quantity of cable required per unit length of load (without terminal lengths) is

$$l_{Ca}^* = N_{Ca}^* \cdot l_{Ca} = \left\{ \frac{\left[\left(\varepsilon\beta + \frac{1-\beta}{2}\right) \cdot \sqrt{\frac{Y}{X}} + \frac{1}{2}\sqrt{\frac{X}{Y}}\right]}{\sqrt{W_m}} - \frac{K_T}{2} \right\} \frac{\sqrt{2}\, \eta\, g\, \alpha_K}{\sqrt{\pi \mu_0}\, \bar{c}_i D C_{Ca} \sqrt{K_S}} \cdot \frac{n^2}{\omega^2} \tag{88}$$

1.8 Example

With the equations derived so far a rapid rise capacitor bank according to Fig. P 176 can be determined, as shown in the following example.

The data given are:

$D = 10$ cm, $A = 100$cm, $\hat{B} = 200$ kG, $\dot{B} \approx 10^{11} \frac{G}{sec}$ (desired),

$\eta = \frac{2}{3}$, $n = 2$

The system called for is one of the infinetely large number of systems described by equation (20). Whether the desired value of $\dot{B}$ can be reached or not depends on the value of K_S.

Possible values are

$c_{Ca} = 0.067 \cdot 10^{-3} \frac{cm}{V}$

$c_o = 0.7 \cdot 10^{-3} \frac{cm}{V}$

$c_d = 0.003 \cdot 10^{-3} \frac{cm}{V}$

$c_i = 0.35 \frac{A}{V}$

$\overline{c_i} = 0.331 \sqrt{\frac{Wsec}{cm^3}}$

$\alpha_k = 0.576$ (for $\eta = \frac{2}{3}$)

$\sqrt{f_{Co}} = 0.5$

$\lambda = 2$

$\beta = 0.5$

$\varepsilon\beta = 0.1$

$K_T = 1.5 \sqrt{\frac{cm^3}{Wsec}}$

$K_b = 0.5 \sqrt{\frac{cm^3}{Wsec}}$

$L_o = 10$ nH (double that of [5])

$U_o = 60$ kV

$W_m = 0.04 \frac{Wsec}{cm^3}$

$L' = 1.2 \frac{nH}{cm}$

$\varrho = 0.9$

$\tau = 0.5$

$\xi = 0.05$

$g^* = 0.025 \frac{1}{cm}$

We get

$$1 - A = \frac{\mu_0}{6} \frac{\tau \xi \varrho c_i^2}{W_m c_k^2 \alpha_k^2} = 0{,}097 \tag{89}$$

$$y = \frac{L'}{2} - \frac{\mu_0}{3} \tau \xi = 0{,}495 \cdot 10^{-9} \frac{Vs}{Acm} \tag{90}$$

$$X = 0{,}56 \cdot 10^{-9} \frac{Vs}{Acm} \tag{91}$$

$$R_{opt} = \frac{y}{X} = \frac{0{,}495}{0{,}560} = 0{,}885 \tag{92}$$

$$\sqrt{Xy} = 0{,}527 \cdot 10^{-9} \frac{Vs}{A} \tag{93}$$

$$B = \frac{c_i}{\alpha_k} \left[\frac{L_0 K_b}{U_0 c_k} + 2\sqrt{\frac{xy}{W_m}} + \left(\frac{\mu_0 \tau}{4} - \frac{L'}{2} \right) K_T \right] \tag{94}$$

$$= \left[0{,}755 + 3{,}20 + 1{,}414 - 0{,}547 \right] \cdot 10^{-9} \sqrt{\frac{scm}{VA}}$$

$$= 4{,}84 \cdot 10^{-9} \sqrt{\frac{scm}{VA}}$$

$$C = 2 \mu_0 \lambda C_d C_0 = 105{,}5 \cdot 10^{-18} \frac{scm}{VA} \tag{95}$$

Thus we have according to equation (70)

$$K_S = 191{,}2 \cdot 10^{-18} \frac{scm}{VA} \tag{96}$$

$$\sqrt{K_S} = 13{,}83 \cdot 10^{-9} \sqrt{\frac{scm}{VA}}$$

and from equation (20)

$$\omega^2 \frac{E^*}{n} = \frac{1-\eta}{K_S} = 17{,}4 \cdot 10^{14} \frac{VA}{sec\,cm} \tag{96a}$$

This now fixes the discharge frequency. With

$$E^* = \frac{\hat{B}^2}{2\mu_0} \frac{\pi}{4} D^2 \frac{1}{\eta} \tag{97}$$

we have

$$\frac{E^*}{n} = 0{,}937 \cdot 10^4 \frac{VA\,sec}{cm} = 0{,}937 \frac{MJ}{m} \tag{98}$$

$$\omega = 4{,}31 \cdot 10^5 \frac{1}{Sec} \tag{99}$$

$$f_o = 68{,}7\ kHz \tag{100}$$

$$\dot{B} = 0{,}862 \cdot 10^{11} \frac{G}{Sec} \tag{101}$$

An increase of $\dot{B}$ would be achieved only for a smaller K_S value, i.e. by improving, if possible, design and technology.

With the aid of equation (74) we have to check whether the figures put into the formula yield a realistic value for the capacitor energy density. We get

$$W_C = \frac{W_m}{\varrho J \left(1 - \frac{2 C_k^2 \alpha_k}{\varrho c_i \sqrt{K_S}} \sqrt{\frac{x}{y} W_m}\right)} = 0{,}115 \frac{Wsec}{cm^3} \tag{102}$$

A usual capacitor design works at 0.065 $\frac{Wsec}{cm^3}$ for 85 % reversal ringing discharges. So the resulting values can be tolerated for about 40 % reversal, which is sufficient for additional passive crowbar or power crowbar application.

The percentage subdivision of the source inductance has already been given in Table I. The corresponding inductances for A = 100 cm are

load coil	L	= 9.86 nH	(103)
capacitor bank	$2\ L_{i2}$	= 4.93 nH	(103a)
capacitors	$2\ L_C$	= 0.355 nH	(103b)
spark gaps	$2\ L_S$	= 0.275 nH	(103c)
cables	$2\ L_{Ca}$	= 0.927 nH	(103d)
cable connections	$4\ L_T$	= 0.512 nH	(103e)
collector	$2\ L_{Co}$	= 2.861 nH	(103f)

The charging voltage becomes from equation (82) (n = 2):

$$U_2 = 50.8 \text{ kV} \tag{104}$$

The total bank energy is with equation (98)

$$E_1 = 1.874 \text{ MJ} \tag{105}$$

The energy of the single capacitor unit from equation (81) becomes

$$E_c = 10.9 \text{ kJ} \tag{106}$$

and therefore the total number of capacitor units

$$N_c^* \cdot A = \frac{E_1}{E_c} = 172 \tag{107}$$

The capacitance of the capacitor unit is according to equations (83) with(104)

$$C_E = 8.5\ \mu\text{F} \tag{108}$$

For the storage block height we have with equation (76)

$$H = 446 \text{ cm} \tag{109}$$

and the (calculated) number of tiers (equation 79) is

$$e = 9.28 \tag{110}$$

thus the height of one tier

$$h_e = 48 \text{ cm} \tag{111}$$

According to equation (67) the depth of one cubic unit becomes

$$T_m = 145 \text{ cm} \tag{112}$$

The bank block depth is

$$T = \frac{H}{R_{opt}} = 505 \text{ cm} \tag{113}$$

and consequently,

$$z = \frac{T}{T_m} = 3.48 \tag{114}$$

(In practice, one would choose e = 9 and z = 4)

the cable diameter is

$$D_{Ca} = c_{Ca} \cdot U_n = 3.4 \text{ cm} \tag{115}$$

Therefore according to equation (39) we have

$$\sigma = 0.755 \tag{116}$$

Now the dimensions of the single capacitor unit are fixed:

$$\text{height} \quad \sigma' \cdot h_e = 36.2 \text{ cm} \tag{117}$$

$$\text{width} \quad \varsigma \cdot \frac{1}{g^*} = 36.0 \text{ cm} \tag{118}$$

$$\text{length} \quad \tau \cdot T_m = 72.5 \text{ cm} \tag{119}$$

The average cable length (without terminal) is according to equation (87)

$$l_{Ca} = 338 \text{ cm} \tag{120}$$

and the total number of cables with equation (84)

$$N^*_{Ca} \cdot A = 1740 \tag{121}$$

i.e. we have per capacitor unit

$$\frac{1740}{172} = 10.1 \text{ cables.}$$

The total length of cable required is (without terminals)

$$1740 \cdot 3.38 \text{ m} = 5900 \text{ m} \tag{122}$$

Some single-component inductances are

capacitor	15.1 nH
spark gap	11.8 nH
cable	402 nH
cable terminal	111 nH

For practical application, the results must be adapted to integer numbers of components and units and to results of design and development. Figure P 182 shows the frequency dependence of some characteristic parameters for systems having the same storage constant as the example calculated. Besides the geometric figures H, $\frac{e}{\sqrt{n}}$, l_{Ca}, $\frac{1}{n^2} \cdot l^*_{Ca}$, the capacitor data $\frac{C_E}{\sqrt{n}}$, $E_c\sqrt{n}$ and the energy per unit length of load $\frac{E^*}{n}$, we have the curve for the ideal maximum instantaneous apparent power per unit length of load $\omega \frac{E^*}{n}$, which is also a measure of the price of a fast capacitor energy storage system. From experience, one can calculate for the power $\omega E^* A$ with a price rate of about $2.5 \frac{\text{\$}}{\text{MVA}}$ without and about $3 \frac{\text{\$}}{\text{MVA}}$ with passive crowbar (including auxiliary equipment and load coil). This means about 2 million dollar for the example. A measure of the passive crowbar ripple is the ratio of the inductances of the crowbar branch and the crowbar circuit. On the assumption that every unit has its crowbar switch with, for instance double inductance compared to the main gap, we get for the example calculated:

$$\frac{2\,L_S + 2\,L_T}{\frac{L}{n} + L_{in} - L_c} = 7.35\ \% \qquad (122a)$$

1.9 Some remarks on K_s

Figure P183 shows the charging voltage versus K_s for D = 10 cm and $\eta = \frac{2}{3}$. The question arises how K_s can be further reduced. The most important parameters in this connection are

$$c_i\ ,\ c_d\ ,\ \text{and}\ c_o$$

H	$\frac{e}{\sqrt{n}}$	$\frac{C_E}{\sqrt{n}}$	l_{ca}	$\frac{1}{n^2}l_{ca}^*$	$\omega\frac{E_n^*}{n}$	$E_c\sqrt{n}$
m		μF	m	$\frac{m}{cm}$	$\frac{VA}{cm}$	VAs
10		10		100	10^{10}	
1	10	1	10	10	10^9	10^5
	1		1	1	10^8	10^4

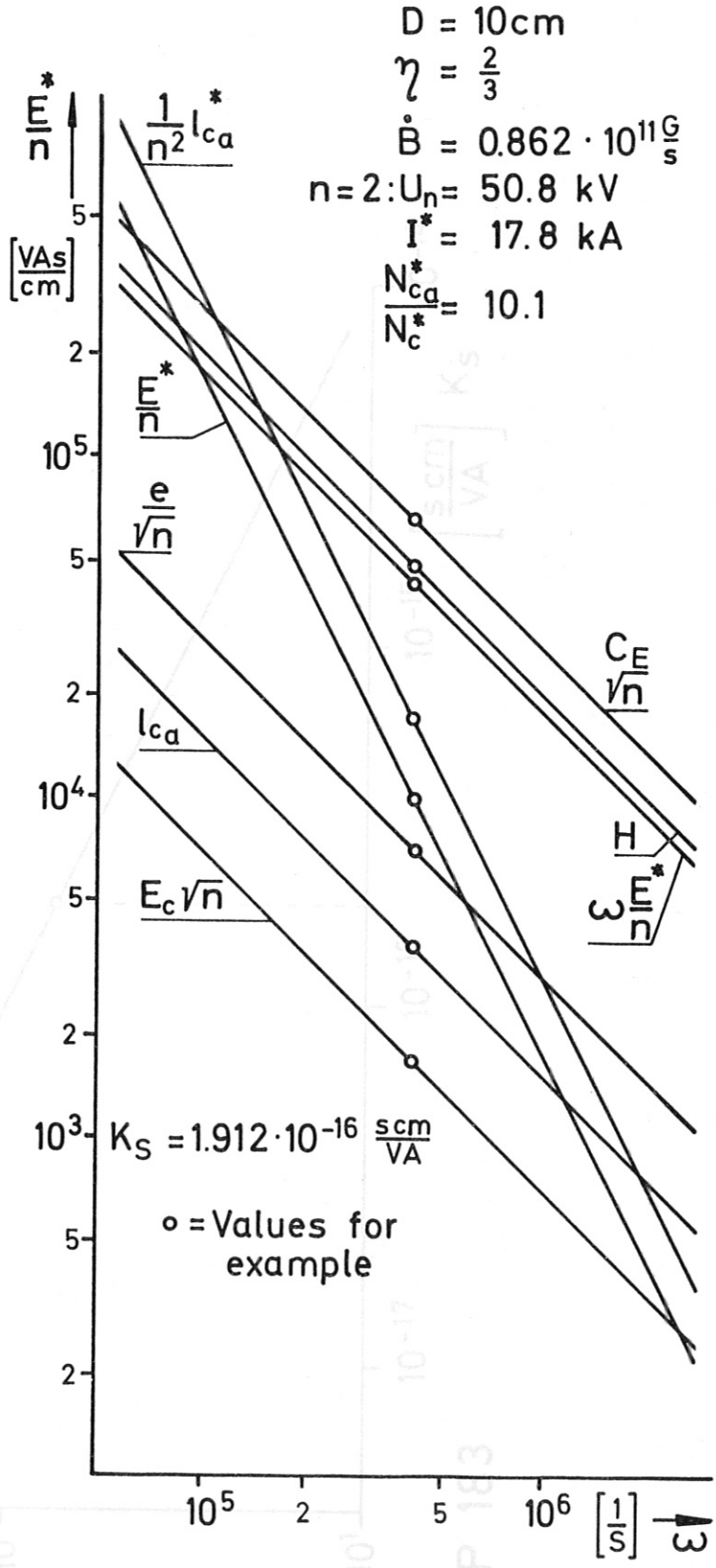

Capacitive Energy Storage
design curves (example)

P 182

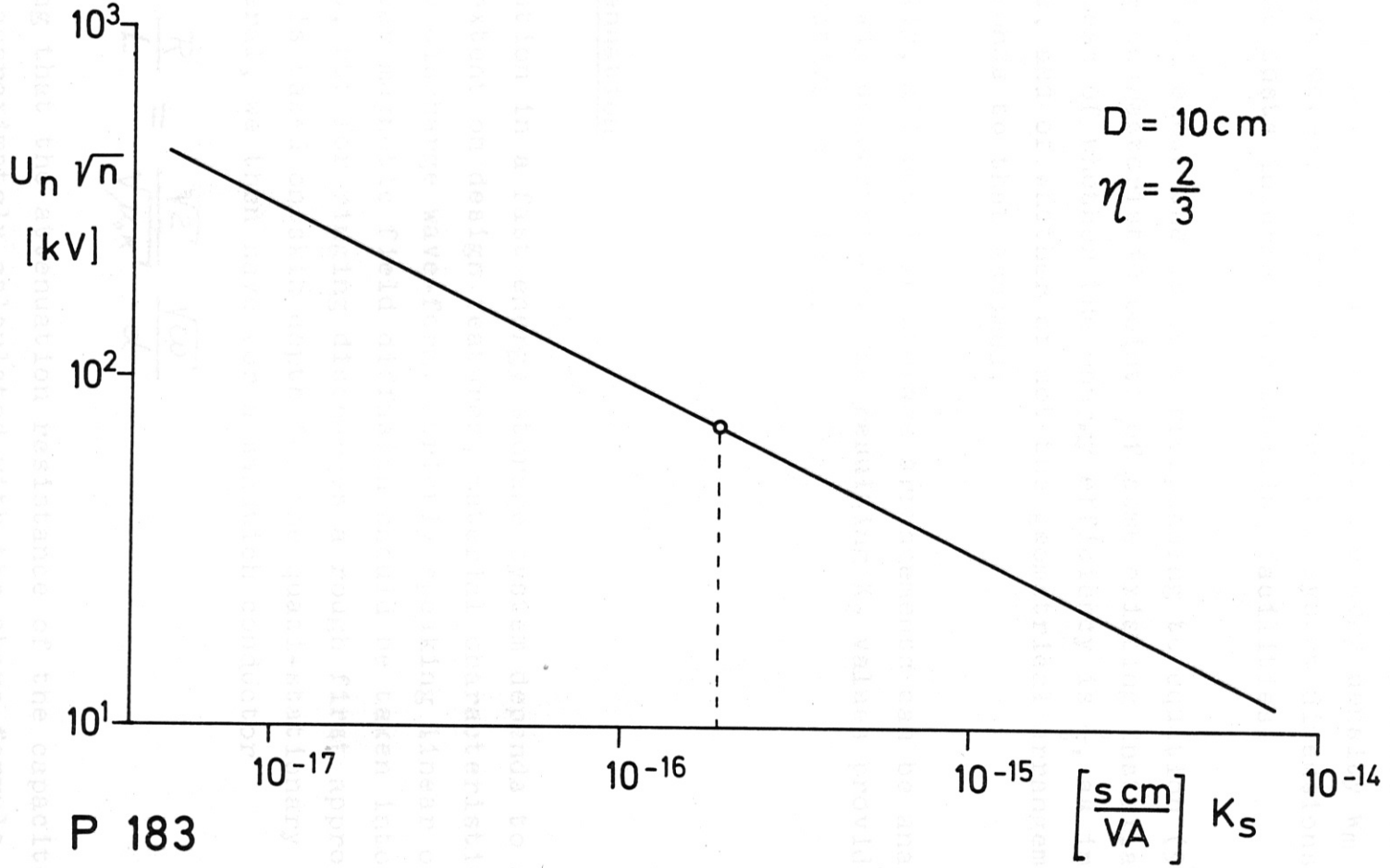
10^3
$U_n \sqrt{n}$
[kV]
10^2
10^1
10^{-17}
10^{-16}
10^{-15}
10^{-14}
$\left[\frac{s\,cm}{VA}\right]$ K_s
D = 10cm
$\eta = \frac{2}{3}$

P 183

i.e. K_S can be greatly reduced by increasing the number of cables and/or, better still, reducing the insulation distances. All remaining parameters have a comparatively small influence on K_S. Even a high effective energy density w_m in the store merely serves to reduce the system dimensions, i.e. the costs incurred for building facilities.

Figure 184 shows the curve corresponding to equation (96a) and the characteristic points of some existing installations, regardless of whether the energy efficiency is $\frac{2}{3}$, as in our example, and of whether or not the geometrical arrangement corresponds to that assumed.

Naturally, all possible storage arrangements can be analyzed in the way demonstrated. The resulting K_S values provide an objective comparison.

2 Attenuation

Attenuation in a fast energy storage system depends to a large extent on design features, material characteristics, and the discharge wave-form. Strictly speaking linear or nonlinear magnetic field diffusion should be taken into account, but for ringing discharges a rough first approximation is based on skin depth for the quasi-stationary state. In general, we then have for a sandwich conductor

$$\frac{R}{L} = \frac{\sqrt{2}}{\sqrt{\mu_0 \kappa}} \frac{\sqrt{\omega}}{d} \qquad (123)$$

Assuming that the attenuation resistance of the capacitors can be approximately calculated with the above formula, taking equation (54) for d and with the use of equations (73b) and (82), we have

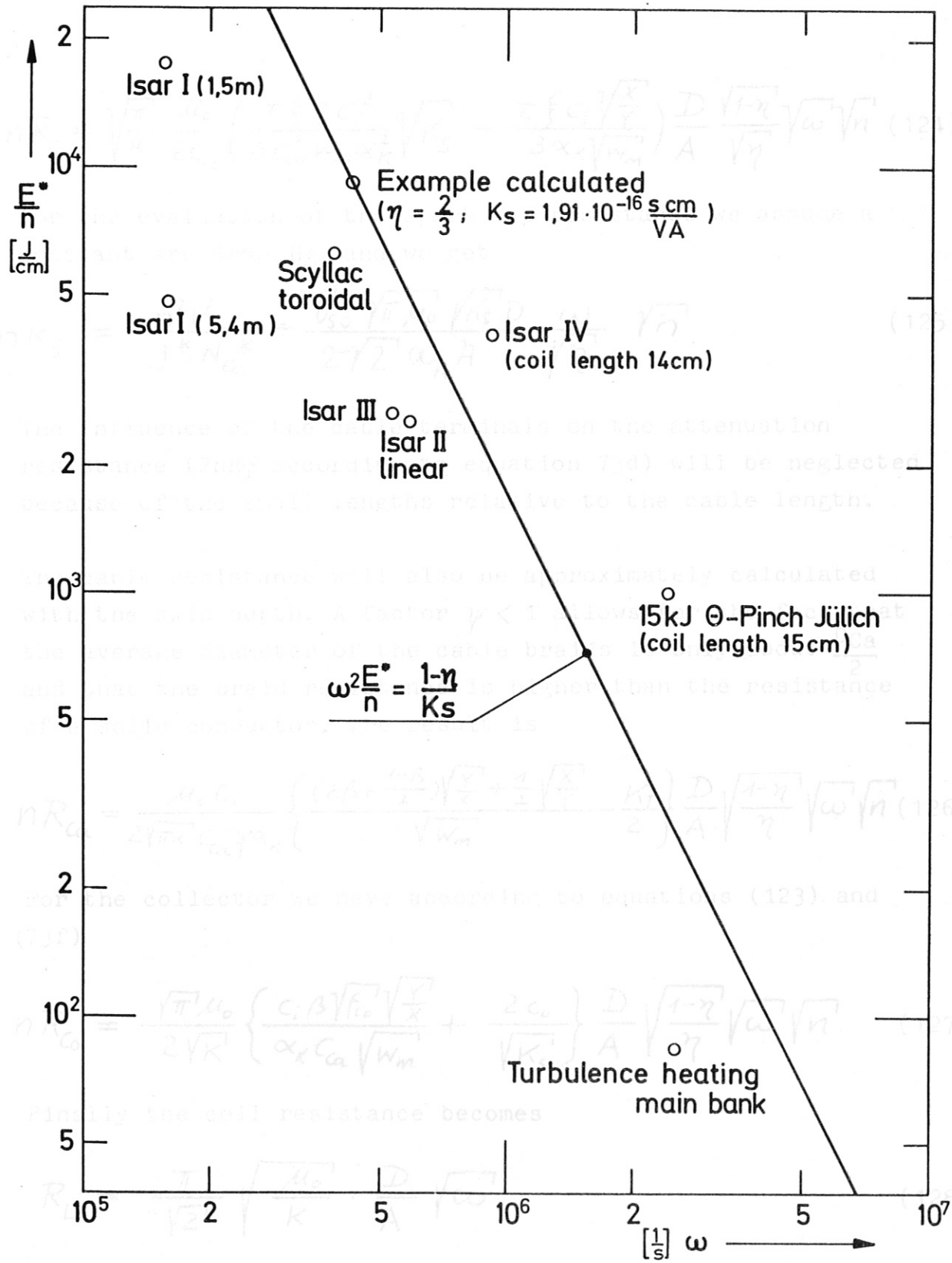

Capacitive Energy Storage

Energy per unit length versus frequency: example and existing installations.

P 184

$$nR_c = \sqrt{\frac{\pi}{K}}\,\frac{\mu_0}{2c_d}\left(\frac{\tau\,\xi\,\varrho\,c_i^2}{6c_{ca}^2 w_m \alpha_K^2}\sqrt{K_s} - \frac{\tau\,\xi\,c_i\sqrt{\frac{X}{Y}}}{3\alpha_K\sqrt{w_m}}\right)\frac{D}{A}\,\frac{\sqrt{1-\eta}}{\sqrt{\eta}}\sqrt{\omega}\sqrt{n} \quad (124)$$

For the evaluation of the spark gap resistance we assume a constant arc drop U_{So} and we get

$$nR_S = \frac{n^2 V_{So}}{J^* N_{ca}^*} = \frac{V_{So}\sqrt{\pi\mu_0}\sqrt{K_s}D}{2\sqrt{2}\,\alpha_K A}\,\frac{\omega}{\sqrt{\eta}}\,\sqrt{n} \quad (125)$$

The influence of the cable terminals on the attenuation resistance ($2nR_T$ according to equation 73d) will be neglected because of the small lengths relative to the cable length.

The cable resistance will also be approximately calculated with the skin depth. A factor $\psi < 1$ allows for the fact that the average diameter of the cable braids is only about $\frac{D_{Ca}}{2}$ and that the braid resistance is higher than the resistance of a solid conductor. The result is

$$nR_{Ca} = \frac{\mu_0 c_i}{2\sqrt{\pi\kappa}\,c_{ca}\psi\alpha_K}\left\{\frac{(\varepsilon\beta + \frac{1-\beta}{2})\sqrt{\frac{Y}{X}} + \frac{1}{2}\sqrt{\frac{X}{Y}}}{\sqrt{w_m}} - \frac{K_T}{2}\right\}\frac{D}{A}\sqrt{\frac{1-\eta}{\eta}}\sqrt{\omega}\sqrt{n} \quad (126)$$

For the collector we have according to equations (123) and (73f)

$$nR_{Co} = \frac{\sqrt{\pi}\mu_0}{2\sqrt{K}}\left\{\frac{c_i\beta\sqrt{f_{Co}}\sqrt{\frac{Y}{X}}}{\alpha_K c_{Ca}\sqrt{w_m}} + \frac{2c_o}{\sqrt{K_s}}\right\}\frac{D}{A}\sqrt{\frac{1-\eta}{\eta}}\sqrt{\omega}\sqrt{n} \quad (127)$$

Finally the coil resistance becomes

$$R_L = \frac{\pi}{\sqrt{2}}\sqrt{\frac{\mu_0}{K}}\cdot\frac{D}{A}\sqrt{\omega} \quad (128)$$

With equations (124) to (128), the distribution of losses is known. Since in plasma experiments the energy input into the plasma is almost negligible, in general, the amount of energy dissipated in the single components is known.

The resistance values for the example (n = 2) calculated are (with U_{So} = 150 V)

load coil	R_L = 21.6 $\mu\Omega$	≙ 8.0 %	(129)
capacitor bank	2 R_{i2} = 249.1 $\mu\Omega$	≙ 92.0 %	(129a)
capacitors	2 R_c = 36.5 $\mu\Omega$	≙ 13.5 %	(129b)
spark gaps	2 R_s = 19.0 $\mu\Omega$	≙ 7.0 %	(129c)
cables (= 0.3)	2 R_{Ca} = 40.4 $\mu\Omega$	≙ 14.9 %	(129d)
collector	2 R_{Co} = 153.2 $\mu\Omega$	≙ 56.6 %	(129e)

This means:

resistance per capacitor unit 2.54 mΩ
total cable resistance per unit length 5.21 $\frac{m\Omega}{m}$

All resistances hold for $\omega = 4.31 \cdot 10^5 \frac{1}{s}$

The decay constant for the ringing discharge of the sample system is

$$T = \frac{2\,(L+2L_{i2})}{R_L+2R_{i2}} = 110\,\mu sec \qquad (130)$$

whereas for crowbarred discharges about

$$T_{Cr} = 55\,\mu sec \text{ will apply.} \qquad (131)$$

With $\delta = \frac{1}{T}$ and equation (123) we get

$$\frac{\delta}{\omega} \sim \frac{1}{\sqrt{\omega}} \qquad (132)$$

i.e. the relative attenuation decreases with increasing frequency. In absolute values of course, the decay constants decrease with increasing frequency of the current rise. Thus, expecially with rapid energy storage systems, a passive crowbar with the crowbar switches adjacent to the main gaps becomes uneconomical. The arrangement of the crowbar switches at the coil, which in the example would ideally yield a crowbar decay constant

$$T_{Cr} = 0.458 \text{ msec}, \qquad (133)$$

involves design problems and requires a relatively small number of heavy-duty switches, e.g. dielectric switches.

3 Generation of constant current period of msec duration

The limit on possible pulse durations with passive crowbar indicated by equation (131) can be overcome with the aid of an active or power crowbar, which means that an additional energy storage system of comparatively low voltage supplies the loss energy during the constant current period.

Figure P 185 shows the desired current programme.

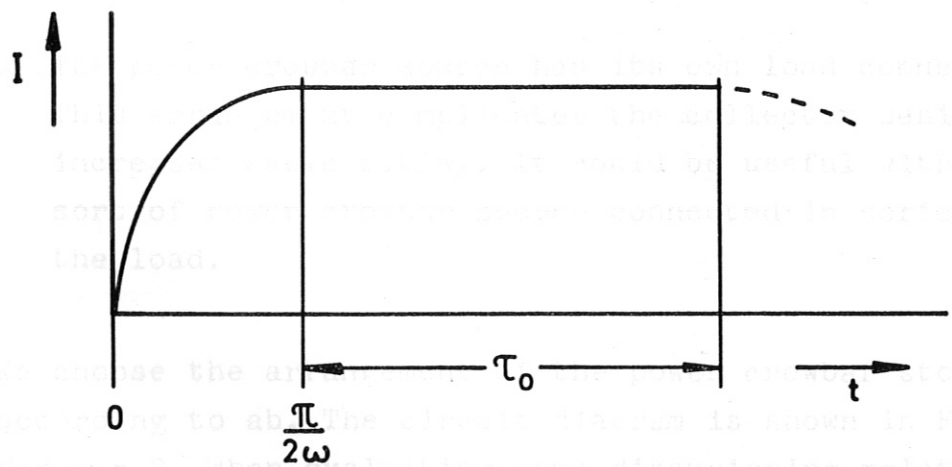

P 185

3.1 Lumped parameter delay line as power crowbar source

The following considerations concern the delay line as one of the possible power crowbar sources.

There are several possibilities of connecting a power crowbar source with the fast rise storage device:

a The pulse cables of the fast capacitor bank are used to connect the power crowbar source to the load.

   aa The fast storage system and delay line form a unit. In this case, the cable lengths are increased according to the volume required for the delay line and any enlargement of the power crowbar source is very difficult.

   ab The delay line system and the fast capacitor bank are connected in tandem with the delay line having the same height H. The cables of the crowbar source are connected to the fast units.

b The power crowbar source has its own load connection. This arrangement complicates the collector design and increases cable outlay. It could be useful with another sort of power crowbar source connected in series with the load.

We choose the arrangement of the power crowbar storage system according to ab. The circuit diagram is shown in Fig. P 186 for n = 2. When evaluating some dimensioning relations for the power crowbar source in terms of the fast circuit data, the following assumptions are made.

1. The power crowbar source is a delay line composed of equal L-networks (C_p, L_p) according to [6]. In analogue model measurements with delay lines containing m = 5 L-networks we could show that the homogeneous lumped parameter line gives better current wave-forms than the equivalent Cauer two-terminal network [7] . Besides this fact, practical reasons favour the homogeneous line.

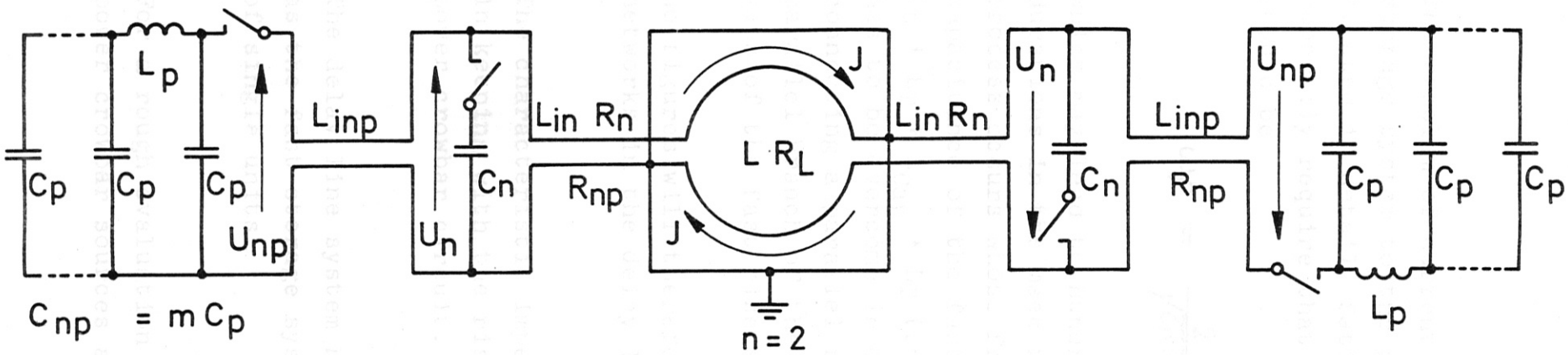

Circuit Diagram

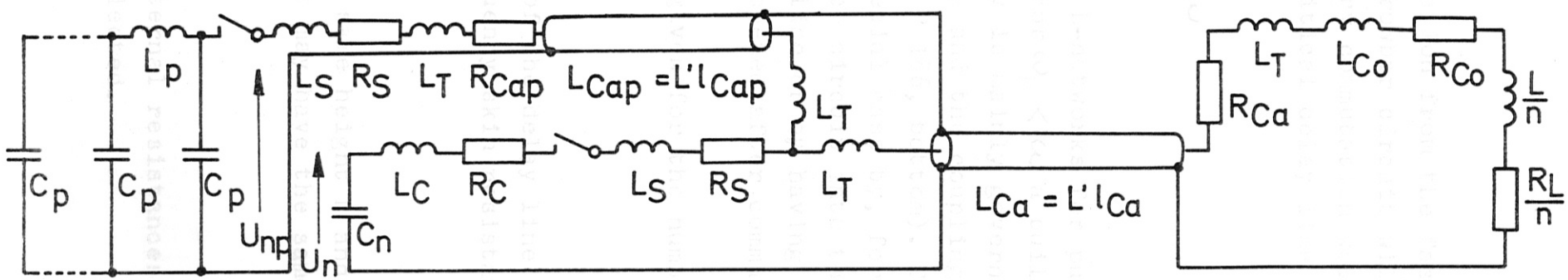

Inductance Components

Capacitive Energy Storage
inductive load, n banks in series with power crowbar

The problem of current commutation from the fast energy storage system to the power crowbar circuit will not be treated in detail. Satisfactory commutation would generally require that the critical delay line frequency should be

$$\omega p = \frac{2}{\sqrt{C_p L_p}} \geq \omega \qquad (134)$$

which may lead to hundreds of L-networks for pulse durations in the msec range. For $\omega_p < \omega$ a building-up process occurs whose frequency is mainly governed by the capacitance of the fast source and the coupling inductance $L_S + L_T + L_{Cap} + L_T$ (see Fig. P 186, bottom). This problem has to be overcome in each special case by, for example, connecting a parallel resonance circuit into the first parallel branch of the delay line or by having the main gaps of the fast rise source opened after commutation.

No figures will therefore be given for the number m of networks in the delay line.

2. The characteristic impedance of the delay line is dimensioned in keeping with the rise frequency skin resistance of the power crowbar circuit.

3. The delay line system has the same height H and width A as the fast storage system. It may have the same number of single units.

4. For a rough evaluation all internal resistances of the power crowbar sources are neglected.

The following relations hold for the pulse duration

$$\tau_0 = 2m\sqrt{L_p C_p} \tag{135}$$

the characteristic impedance

$$Z_n = \sqrt{\frac{L_p}{C_p}} \tag{136}$$

From these equations we have

$$C_{np} = mC_p = \frac{\tau_0}{2Z_n} \tag{137}$$

The matching condition for the impedance is

$$Z_n = R_{ca} + R_{co} + \frac{R_L}{n} \tag{138}$$

and for the currents

$$\frac{U_{np}}{2Z_n} = U_n\sqrt{\frac{nC_n}{L + nL_{in}}} \tag{139}$$

So the power-crowbar charging voltage becomes

$$U_{np} = 4\sqrt{\frac{2}{\pi K}}\, M(n)\, \frac{\sqrt{\eta(1-\eta)}}{\sqrt{K_s}}\, \frac{1}{\sqrt{\omega}} \tag{140}$$

with

$$M(n) = \frac{\sqrt{\mu_0}}{2\sqrt{\pi}}\, \frac{C_i}{\psi a_K C_{ca}} \left\{ \frac{(\varepsilon\beta + \frac{1-\beta}{2})\sqrt{\frac{Y}{X}} + \frac{1}{2}\sqrt{\frac{X}{Y}}}{\sqrt{w_m}} - \frac{K_T}{2} \right\} \tag{141}$$

$$+ \frac{\sqrt{\mu_0}\sqrt{\pi}}{2} \left\{ \frac{C_i \beta \sqrt{f_{co}}\sqrt{\frac{Y}{X}}}{a_K \sqrt{w_m}\, C_{ca}} + \frac{2c_o}{\sqrt{K_s}} \right\} + \frac{\pi}{\sqrt{2}}\, \frac{1}{\sqrt{n}}$$

which results from uniform representation of equations (126) to (128):

$$n\left(R_{Ca} + R_{Co} + \frac{R_L}{n}\right) = M(n)\sqrt{\frac{\mu_o}{K}}\,\frac{D}{A}\sqrt{\omega}\sqrt{n} \qquad (142)$$

As the contribution of the load coil to the total attenuation resistance is comparatively small, M(n) depends only weakly on n. Therefore equation (140) yields a value of the charging voltage that is almost independent of n. The delay line energy becomes

$$\frac{E^*_p}{n} = \frac{m C_p U_{np}^2}{2} \qquad (143)$$

and with equation (140)

$$\frac{E^*_p}{n} = \frac{8}{\pi}\,\frac{\tau_o}{D}\,\frac{M(n)}{\sqrt{\mu_o K}}\,\eta\,\frac{E^*}{n}\sqrt{\omega}\sqrt{n} \qquad (144)$$

or

$$\frac{E^*_p}{n} = \frac{8}{\pi}\,\frac{\tau_o}{D}\,\frac{M(n)}{\sqrt{\mu_o K}}\,\frac{\eta(1-\eta)}{K_s}\,\frac{\sqrt{n}}{\omega^{\frac{3}{2}}} \qquad (145)$$

For the calculated example we get according to equation (140) a charging voltage of

$$U_{2p} = 3.43 \text{ kV} \qquad (146)$$

with M(2) = 15.62 (= 2.93 + 11.12 + 1.57) (147)

For a pulse duration τ_o = 200 µsec we get with equation (144)

$$E^*_p = 5.81 \cdot E^* \qquad (148)$$

i.e. a power crowbar installation according to Fig. P 186 with a fast rise storage system entails, even for pulse durations in the 0.1 msec range, considerable outlay. It should be noted that in our example the amount of energy for the coil alone is only 0.584 E^*.

3.2 Influence of magnetic field diffusion

In reality, the situation may be much more favourable than that resulting from relation (148), because the magnetic field and, at the same time, the current penetrates into the conductors during the time interval τ_o, and so the effective resistance decreases. From a calculation of Kidder [8] it can be shown that the equivalent conducting sheath for a penetrating constant magnetic field with an infinitely steep initial rise is given by

$$\delta_{diff} = 0{,}63 \frac{2\sqrt{t}}{\sqrt{\mu_o \kappa}} \qquad (149)$$

Figure P 187 shows the loop of δ_{diff} for copper.

The calculated values for U_{np} are thus valid only for the starting time of the constant current period τ_o. Up to this time a conducting sheath of

$$\delta_{rise} = \sqrt{\frac{2}{\omega \kappa \mu_o}} \qquad (150)$$

has formed according to our approximation of equation (123).

Equations (149) and (150) are set equal. Thus a replacement switching time t_o is found, from which the field diffusion according to equation (149) starts. We get

$$t_o = \frac{1{,}26}{\omega} \qquad (151)$$

Consequently, the time dependent voltage required for the constant current circuit is found from equations (140) and (151) to be

$$U_{npdiff} = 2\sqrt{\frac{2}{\pi\kappa}} \cdot \frac{\Gamma}{\lambda} M(n) \frac{\sqrt{\eta(1-\eta)}}{\sqrt{K_s}} \cdot \frac{1}{\sqrt{\omega}} \sqrt{\frac{1{,}26}{\omega t}} \qquad (152)$$

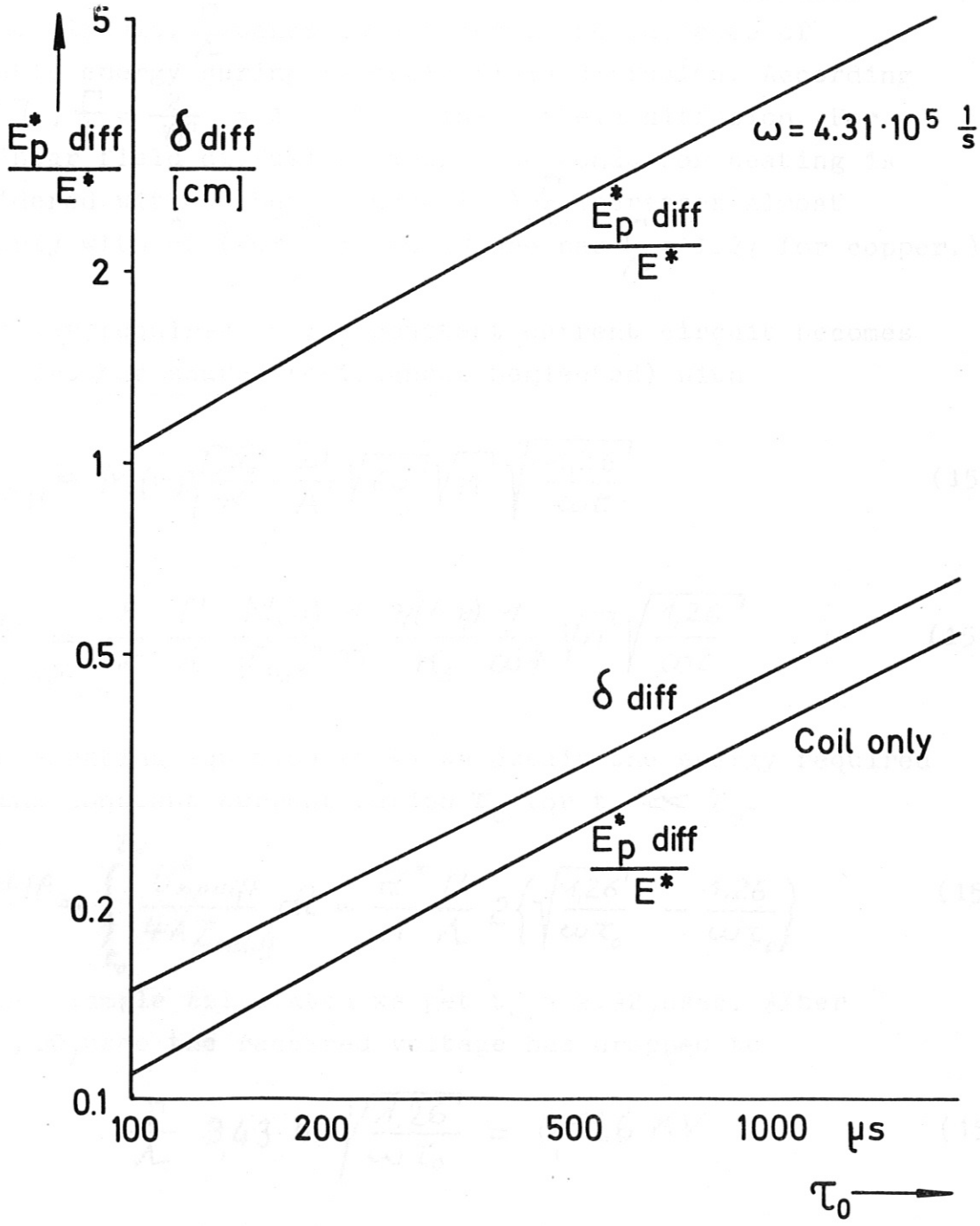

Capacitive Energy Storage

Energy relation for power crowbar source to fast rise source and equivalent conducting sheath versus pulse duration

P187

This equation and all following relations hold in good approximation as long as the equivalent conducting sheath does not attain the actual conductor thickness anywhere in the circuit. $\frac{\Gamma}{\Lambda}$ takes into account the increase of magnetic energy during magnetic field diffusion. According to [8], $\frac{\Gamma}{\Lambda} = \frac{2}{\sqrt{\pi}} = 1.13$ for linear field diffusion. For nonlinear field diffusion (where the conductor heating is considered without heat conduction) $\frac{\Gamma}{\Lambda}$ increases almost linearly with $\hat{B}$. (For $\hat{B}$ = 200 kG one has $\frac{\Gamma}{\Lambda} = 1.27$ for copper.)

The power required in the constant current circuit becomes (with crowbar source resistances neglected) with

$$n Z_{ndiff} = M(n)\sqrt{\frac{\mu_0}{\kappa}} \cdot \frac{D}{A}\sqrt{\omega}\sqrt{n}\sqrt{\frac{1{,}26}{\omega t}} \tag{153}$$

$$\frac{U^2_{npdiff}}{4A Z_{ndiff}} = \frac{8}{\pi}\frac{\Gamma}{\Lambda}\frac{M(n)}{\sqrt{\mu_0 \kappa}}\frac{1}{D}\frac{\eta(1-\eta)}{K_s}\frac{1}{\omega^{\frac{3}{2}}}\sqrt{n}\sqrt{\frac{1{,}26}{\omega t}} \tag{154}$$

By integrating equation (154) we obtain the energy required for the constant current period τ_0 for $t_0 \ll \tau_0$.

$$\frac{E^*_{p\,diff}}{n} = \int_{t_0}^{\tau_0} \frac{U^2_{npdiff}}{4A Z_{ndiff}}\,dt = \frac{E^*}{n}\frac{\Gamma}{\Lambda} 2\left\{\sqrt{\frac{1{,}26}{\omega\tau_0}} - \frac{1{,}26}{\omega\tau_0}\right\} \tag{155}$$

In the example calculated we get t_0 = 2.92 µsec. After τ_0 = 200 µsec the required voltage has dropped to

$$\frac{\Gamma}{\Lambda}\ 3{,}43\ KV\sqrt{\frac{1{,}26}{\omega\tau_0}} = 0{,}526\ KV \tag{156}$$

and consequently the energy required up to τ_0 has decreased to

$$\frac{E^*_{p\,diff}}{n} = 1{,}58\ \frac{E^*_p}{n} \tag{157}$$

The coil alone requires 0.159 · E^*.

It can be seen that there is a considerable reduction of the energy requirements with magnetic field diffusion.

Figure P 187 shows for the sample data the curve E^*_{pdiff}/E^* versus pulse duration τ_o. The additional energy for the period τ_o of a fast rise pulse increases roughly as τ_o. The equivalent conducting sheath, which is also drawn in Fig. P 187, indicates the practical limitation to which the utilization of field diffusion is subject.

The generation of rapid rise current pulses in the msec range by means of two storage systems feeding the same coil can thus be summarized at this stage as follows:

1. Utilization of resistance reduction by magnetic field diffusion affords prospects of economical solutions, especially if losses can be reduced to the order of magnitude of the unavoidable coil losses. It should be borne in mind that economic considerations may be less important for small installations.

2. A power crowbar source must be developed which can generate a constant current output the desired voltage waveform and which has sufficiently low internal losses.

3. This involves, among other things, the development of extremely low-resistance switches designed in such a way that field diffusion can occur in the region of the switch as well.

3.3 Different kinds of power crowbar sources.

3.3.1 Sequentially switched capacitors

A possible power crowbar source with sequentially switched capacitors is shown in Fig. P 188. The different charging

voltages of the capacitors are chosen in keeping with the voltage waveform required with field-diffusion. The amount of energy required would be of the order given by equation (155). One problem is the large number of switches required for a tolerable current ripple [9] .

3.3.2. Variable inductance

This principle is described in Fig. P 189. A variable inductance ($\frac{dLv}{dt} < o$) is connected in series with the load coil. In the first current maximum generated by the fast energy source, the crowbar switch closes and the mechanically driven variable inductance decreases. Initially L_v stores an energy of $\frac{1}{2}L_vJ^2$. Ideally, a total energy of L_vJ^2 can be delivered. Considering the field diffusion, the mechanically delivered part of energy is somewhat larger. In principle, rotating as well as explosively driven devices are possible. [10], [11]

3.3.3 MHD pulse generator

Pulsed MHD generators are being developed, but one has to take into account considerable design difficulties, even from the point of view of geometry. With a magnetic field of 20 kG a power of about 10^9 W per m^2 channel cross sectional area can be expected. By increasing the magnetic field with superconducting coils it should be possible to attain 10^{10}W per m^3. This corresponds roughly to the initial power requirements per m coil length in our example. The length of pulsed MHD channels results from plasma velocities of about $10^4 \frac{m}{sec}$, and so a generator for 1 msec pulse duration would be at least 10 m long [12].

4. Summary

The relations between geometric requirements and electrical data for fast capacitive energy storage systems with inductive load have been derived for a defined arrangement. A kind of "natural" dependence of energy and discharge frequency results.

Furthermore, the amount of energy required for the generation of current pulses in the msec range with respect to the fast rise source is evaluated. Finally, some possible solutions for power crowbar sources are briefly discussed.

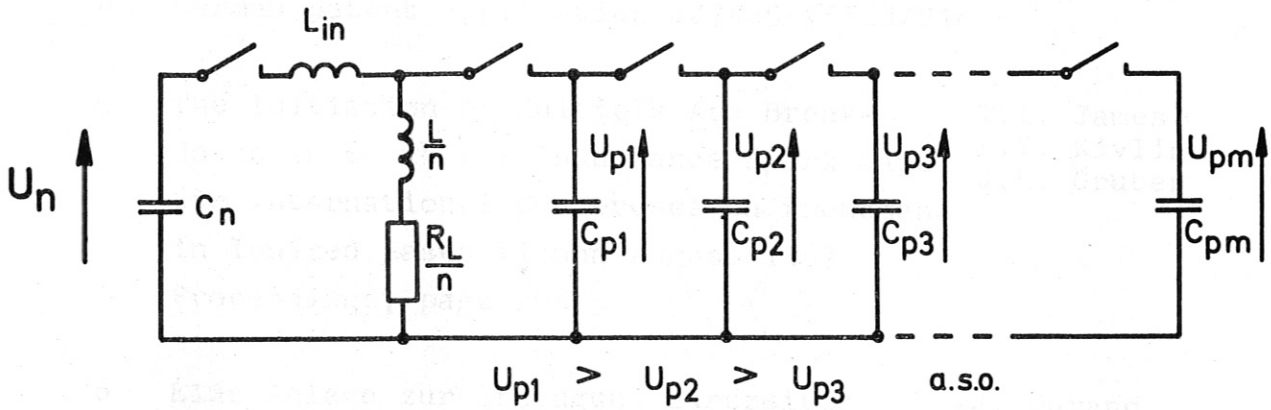

P 188

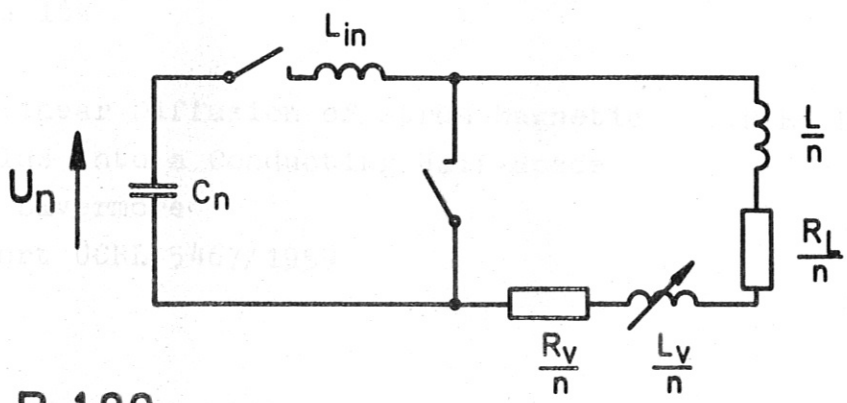

P 189

References:

1 New Fast Capacitor Banks for Theta Pinch Experiments at the Institut für Plasmaphysik in Garching
Report 4/26 1966 IPP Garching
K.H. Fertl
G. Herppich
A. Knobloch
H. Schlageter

2 Personal communication
E. Fünfer

3 Der Kondensatorenergiespeicher als Energiequelle für die Speisung des Theta Pinch Experiments
Unpublished paper 1964
A. Knobloch

4 German patent application J27465 VIIId/21c

5 The Initiation of Multiple Arc Breakdowns in 60 kV Low Inductance Spark Gaps
8th International Conference on Phenomena in Ionized Gases Vienna August 1967
Proceedings, page 208
T.I. James
F.Y. Kivlin
J.E. Gruber

6 Eine Anlage zur Erzeugung kurzzeitig konstanter, starker Magnetfelder
Zeitschr. f. angew. Physik 1960 S. 393
J. Durand
O. Klüber
H. Wulff

7 Pulse Generators
McGraw-Hill 1948
page 189
Glasoe
Lebacqz

8 Nonlinear Diffusion of Stron Magnetic Fields into a Conducting Half-Space
LRL Livermore
Report UCRL 5467/1959
R.E. Kidder

9	The Generation of Large Currents of Constant Amplitude Using Capacitor Banks 3rd Symposium on Engineering Problems in Thermonuclear Research Munich 1964	J. Beraud B. Taquet
10	Vorstudie zu Isar X Unpublished report 1967	A. Knobloch
11	Electrical Pulses from Helical and Coaxial Explosive Generators Proceedings of the Conference on Megagauss Magnetic Field Generation by Explosives and Related Experiments Euratom, Brussels 1966 page 451	D.B. Cummings M.J. Morley
12	Explosive Driven Linear MHD-Generators Proceedings of the Conference on Megagauss Magnetic Field Generation by Explosives and Related Experiments Euratom, Brussels 1966 page 349	M.S. Jones C.N. McKinnon